*Meteoritics & Planetary Science* 40, Nr 9/10, 1493–1511 (2005)
Abstract available online at http://meteoritics.org

# Bosumtwi impact structure, Ghana: Geochemistry of impactites and target rocks, and search for a meteoritic component

Xiongxin DAI[1, 4], Daniel BOAMAH[1], Christian KOEBERL[1*], Wolf Uwe REIMOLD[2], Gordon IRVINE[3], and Iain McDONALD[3]

[1]Department of Geological Sciences, University of Vienna, Althanstrasse 14, A-1090 Vienna, Austria
[2]Impact Cratering Research Group, School of Geosciences, University of the Witwatersrand, P. O. Wits, Johannesburg 2050, South Africa
[3]Department of Earth Sciences, Cardiff University, P.O. Box 914, Cardiff CF10 3YE, United Kingdom
[4]Current address: Department of Physics, Queen's University, Stirling Hall, Queen's Crescent, Kingston, Ontario K7L 3N6, Canada
*Corresponding author. E-mail: christian.koeberl@univie.ac.at

*(Received 20 January 2005; revision accepted 13 July 2005)*

**Abstract**–Major and trace element data, including platinum group element abundances, of representative impactites and target rocks from the crater rim and environs of the Bosumtwi impact structure, Ghana, have been investigated for the possible presence of a meteoritic component in impact-related rocks. A comparison of chemical data for Bosumtwi target rocks and impactites with those for Ivory Coast tektites and microtektites supports the interpretation that the Bosumtwi structure and Ivory Coast tektites formed during the same impact event. High siderophile element contents (compared to average upper crustal abundances) were determined for target rocks as well as for impactites. Chondrite-normalized (and iron meteorite-normalized) abundances for target rocks and impactites are similar. They do not, however, allow the unambiguous detection of the presence, or identification of the type, of a meteoritic component in the impactites. The indigenous siderophile element contents are high and possibly related to regional gold mineralization, although mineralized samples from the general region show somewhat different platinum-group element abundance patterns compared to the rocks at Bosumtwi. The present data underline the necessity of extensive target rock analyses at Bosumtwi, and at impact structures in general, before making any conclusions regarding the presence of a meteoritic component in impactites.

## INTRODUCTION

The 10.5 km in diameter, 1.07 Ma old, and centered at 06°30′N and 01°25′W Bosumtwi crater in Ghana is a well-preserved, complex impact structure. It displays a pronounced rim, but its interior is almost completely covered by Lake Bosumtwi. The crater structure was excavated in metamorphic and igneous rocks of the 2.1–2.2 Ga old Birimian Supergroup. The pronounced crater is surrounded by a slight, near-circular depression, which, in turn, is surrounded by an outer zone of several shallow topographic elevations extending to 9–11 km from the crater center (Jones et al. 1981; Reimold et al. 1998; Wagner et al. 2001; Pesonen et al. 2003).

The crater has been inferred to be the source crater for the Ivory Coast tektites (Fig. 1a), based on the geographical proximity to this tektite strewn field, very similar ages of the crater and tektites, and comparable chemical and isotopic compositions of the tektites and the lithologies occurring in the crater area (Koeberl et al. 1998 and references therein). Thus, the Bosumtwi crater is one of only three impact structures that have been identified as source craters of a tektite strewn field.

Recently, research has been intensified with regard to a number of aspects of the Bosumtwi crater. This includes studies of the petrology and geochemistry of the target rocks (Koeberl et al. 1998), structural analysis of the crater rim (Reimold et al. 1998), a high-resolution aerogeophysical survey including measurements of the total magnetic field, electromagnetic field, and gamma radiation measurements across the structure (Plado et al. 2000; Pesonen et al. 2003), shallow drilling outside the crater rim (Boamah and Koeberl 2003), geochemistry of soils and their relationship to radiometric airborne geophysical data (Boamah and Koeberl 2002), gravity measurements around the lake, and seismic studies that led to the identification of a (buried) central uplift (Karp et al. 2002; Scholz et al. 2002), sediment coring in Lake Bosumtwi (Peck et al. 2004), and a remote-sensing

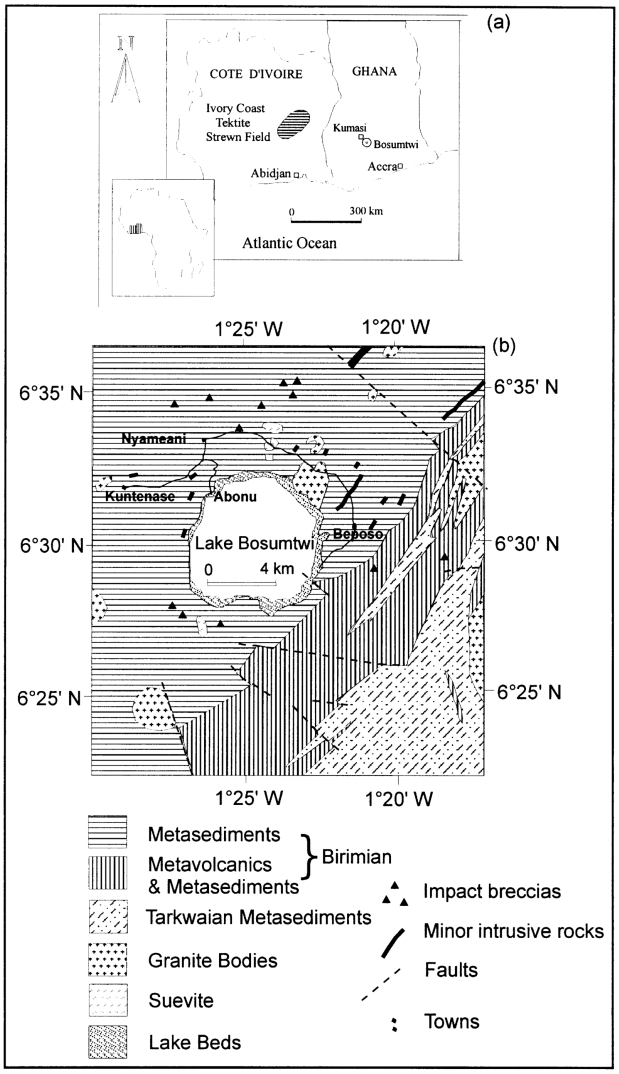


Fig. 1. a) Geographic location of the Bosumtwi impact crater, Ghana, in relation to the Ivory Coast tektite strewn field, and b) schematic geologic map of the area around Lake Bosumtwi; after Koeberl et al. (1998).

investigation (Wagner et al. 2002). In addition, a large international and interdisciplinary drilling effort took place at Bosumtwi during the second half of 2004 (e.g., Koeberl et al. 2005), during which a long, continuous section through the crater fill and underlying basement was retrieved.

Here, we focus on multi-element chemical analyses of target rocks and impact-derived rocks (impactites), and discuss problems with the identification of a meteoritic component at Bosumtwi.

## METEORITIC COMPONENT IN BOSUMTWI ROCKS

The presence of a meteoritic component in impactites is often difficult to establish, and such a component may be difficult to distinguish from the composition of the target rocks because only small quantities of meteoritic matter are mixed with the target rocks (Pernicka et al. 1996; Koeberl and Shirey 1997; Koeberl 1998). Only elements that are very abundant in meteorites but are of low abundance in crustal rocks, such as the siderophile elements, and especially the platinum group elements (PGEs), can be used to detect a meteoritic component. In addition, it must be ascertained that no mantle-derived component, or any other indigenous component, contributes to the target rock composition.

El Goresy (1966) reported the presence of microscopic metallic spherules in glass in Bosumtwi suevite, with a composition similar to that of kamacite in meteorites, with 95.4 wt% Fe, 5.4 wt% Ni, and 0.6 wt% Co. Jones et al. (1981) stated that Ni concentrations in stream sediments from the region inside the slightly elevated zone around Bosumtwi were generally higher than those of Birimian rocks from the wider environs. These authors suggested that this enrichment could represent the presence of meteoritic material—a reasonable assumption as widespread occurrence of suevite in this zone had been established by then. Palme et al. (1978) measured the concentrations of the siderophile elements Ir, Os, Ni, Pd, and Ge in an Ivory Coast tektite sample. They reported that its Ir content of 0.33 ppb was significantly higher than terrestrial crustal values and, hence, that it constituted a meteoritic signature. Based on observations of Ni-Fe spherules in impact glass in suevite, variable Ni and high Ir concentrations in the tektites, and anomalously high Ni in stream sediments at Bosumtwi, Jones et al. (1981) suggested an iron meteoritic projectile as the impactor of the Bosumtwi impact event (as did Palme et al. 1978, 1981b). However, the target rocks could also have contributed significant Ir, as the Bosumtwi crater occurs in a region known for its extensive gold-sulfide mineralization (Jones 1985). High Ni content (Jones 1985; Koeberl et al. 1998) is also known from the Pepiakese granite body in the immediate vicinity of the crater (Fig. 1b).

The question regarding the presence of a meteoritic component at Bosumtwi was only resolved in a Re-Os isotopic study by Koeberl and Shirey (1993), who found a distinct though very small meteoritic component (≤0.6%, chondritic composition) in Ivory Coast tektites. These authors also found that some samples of the Bosumtwi target rocks had elevated contents of the siderophile elements (e.g., Os), but that the Os isotopic signature in these samples was terrestrial, in contrast to the clear extraterrestrial Os component in Ivory Coast tektites and impact glass fractions from suevites.

## GEOLOGY AND SAMPLES

Detailed geological studies of the region around Lake Bosumtwi have been carried out since the 1930s (Junner 1937; Woodfield 1966; Moon and Mason 1967; Jones et al. 1981; Reimold et al. 1998). A new geological map of Bosumtwi with detailed explanations on the geology of the crater and its environs was recently compiled by Koeberl and

Reimold (2005). Figure 1b schematically introduces the geology around Lake Bosumtwi. In the following paragraphs, we provide a short summary of the geological background of the rocks at Bosumtwi.

The Bosumtwi impact crater was excavated in lower greenschist facies metasediments of the 2.1–2.2 Ga Birimian Supergroup (cf. Wright et al. 1985; Leube et al. 1990; Yao and Robb 1998). These supracrustals comprise interbedded phyllites and mica-schists, meta-tuffs, meta-greywacke, quartzitic greywacke, and shales and slates. Tarkwaian clastic sedimentary rocks, which are regarded as detritus derived from Birimian rocks (Leube et al. 1990), occur east and southeast of the crater (Fig. 1b).

Several Proterozoic granitic intrusions occur in the region around the crater, and some in part strongly weathered dikes of granitic composition have been observed in road cuts in the crater rim (Junner 1937; Woodfield 1966; Moon and Mason 1967; Jones 1985; Reimold et al. 1998). Some of these apparently granitic dikes have an aplitic field appearance, others seem to have a fabric (Reimold et al. 1998). Evidence for layering and grain size variations has also been observed at the thin section scale. In addition, such samples may display, on the thin section scale, pockets of granophyric or spherulitic melt, or even appear to consist entirely of such melt. The origin of these materials is still unresolved, but such samples can be described as locally brecciated and melted greywacke and have been designated as such ("locally melted greywacke") in this investigation. However, it should be noted that these dike formations must be further investigated to clarify their genesis and possible relationship with the impact event. They could represent partially melted sedimentary material, impact breccia injections, or even granitic intrusions that are charged with partially assimilated-locally melted meta-sedimentary xenoliths.

One sample, LB-28, of one of these dikes has a homogeneous microgranitic, though K-feldspar porphyritic texture. As it is texturally distinct from the other samples collected from such dikes, this sample is considered in the following separately from the so-called locally melted greywacke specimens.

The Pepiakese granite complex to the northeast of the crater (Fig. 1b) has been related to the Kumasi batholith to the north of the crater (Moon and Mason 1967). Reimold et al. (1998) estimated the overall granitoid component in the region at no more than 2%. In addition, a few occurrences of dikes of dolerite, amphibolite, and intermediate rocks have been noted. Recent rock formations include the Bosumtwi lake beds, as well as soils and breccias associated with the formation of the crater (Junner 1937; Kolbe et al. 1967; Woodfield 1966; Moon and Mason 1967; Jones et al. 1981; Jones 1985; Koeberl et al. 1997; Reimold et al. 1998) or with erosion of the crater rim.

Abundant but scattered suevite deposits have been observed just outside the northern and southwestern crater rim (Fig. 1b). These breccia deposits played a crucial role in the early attempts to explain the origin of the Bosumtwi crater. Early Bosumtwi workers described this rock as volcanic agglomerate or tuff, and the formation of the crater as a product of endogenic processes (Jones et al. 1981). The recognition of target rock fragments of all stages of shock metamorphism in this lithology, including vitreous and devitrified impact glass, confirmed the impact origin of the breccia and, by implication, of the Bosumtwi crater (Koeberl et al. 1998, and review in Koeberl and Reimold 2005).

The suevite is a medium- to coarse-grained, polymict impact breccia, which is grayish in color and contains abundant fragments of partially altered, glassy melt. The clast population is polymict and comprises both meta-sedimentary rock fragments (schist, shale, phyllitic rocks, greywacke, quartzite) and granitoid-derived clasts. Suevite (specifically melt clasts in suevite) has been used to date the impact event, by application of the K-Ar, fission track, and $^{40}Ar$-$^{39}Ar$ techniques (Koeberl et al. 1997, and references therein). For example, Koeberl et al. (1997) obtained a fission-track age of $1.03 \pm 0.11$ Ma for impact glass from suevite. This is identical to the age obtained for Ivory Coast tektites ($1.05 \pm 0.11$ Ma), supporting the earlier suggestion that the Bosumtwi event is the source of the Ivory Coast tektites (Koeberl et al. 1997).

For the present geochemical investigation, major and trace element abundances were determined for suevite samples from shallow drill cores, impact glass fragments separated from suevite collected at surface exposures, and for samples of the various country rocks at Bosumtwi. In addition, several dike samples obtained along the crater rim section described by Reimold et al. (1998) have been analyzed. Short descriptions of the samples of this study are presented in Table 1.

In addition, a selection of ore mineralized samples (courtesy of R. Klemd) from gold mines in the crater region, from lithologies that are part of the target rocks at Bosumtwi, were analyzed for comparison by ICP-MS (see below). Such ore mineralized rocks might have been present among the target rocks when the Bosumtwi impact occurred and thus might have been incorporated in the impact breccias, as already suggested by Jones (1985).

Samples A1, A2, A2-2, and ASH 2 (quartz mica schist) are all metapelites from the Ashanti mine (e.g., Oberthür et al. 1994). They form the immediate country rock hosting gold-sulfide-bearing quartz veins. These schists consist of varying proportions of quartz, muscovite, biotite, carbonate, and graphite, and are strongly sulfidized. Sulfides (up to 5 vol%) are predominantly arsenopyrite (about 95 vol% of the opaque minerals), which may contain inclusions of pyrrhotite, chalcopyrite, pyrite, marcasite, sphalerite, graphite, and gold. All of the sulfides also occur as matrix minerals. In addition, gold occurs as small grains (<5 μm) in the matrix and shows a fineness between 817 and 820. Further accessories are graphite, zircon, and apatite.

Table 1. Petrographic observations on rocks from the Bosumtwi impact structure.

| Sample No. | Location | Rock type | Description |
|---|---|---|---|
| LB-6 | 6°33.1′N 1°25.9′W | Schist | Very fine-grained, with few clasts of quartz, plagioclase, opaques, and very small flakes of biotite; unshocked. |
| LB-7 | 6°33.2′N 1°25.7′W | Schist | Composed of quartz, plagioclase, and biotite porphyroblasts/clasts; unshocked. |
| LB-8 | 6°33.1′N 1°25.6′W | Meta-sandstone | Cataclastic breccia; plagioclase-rich, with a lot of muscovite flakes; micro-faulting; unshocked. |
| LB-12 | 6°33.1′N 1°25.6′W | Graywacke | Granitic composition; contains relatively large clasts of biotite-schist and large, granite-derived biotite grains; unshocked. |
| LB-17 | 6°33.0′N 1°25.6′W | Graywacke | Quartz-rich; contains some schist clasts; transected by many late, silica-filled veinlets that predate a still later annealing event; unshocked. |
| LB-22 | 6°32.7′N 1°29.7′W | Graywacke (foliated) | Contains a polymict clast population, dominated by granitoid and granitoid-derived mineral clasts; also meta-sediment (schist, chert) clast components; unshocked; clasts are angular to subrounded. |
| LB-37 | 6°30.9′N 1°20.6′W | Phyllite | Greenish, strongly foliated, chlorite-rich phyllite; transected by numerous quartz veins (excluded from analyzed sample suite). |
| LB-19 | 6°32.7′N 1°29.7′W | Graywacke (?) | Locally melted graywacke (?), laminated with patches of granophyric melt texture; possibly related to the "biotite granitoid" dikes of Reimold et al. (1998). |
| LB-21 | 6°32.7′N 1°29.7′W | Graywacke (?) | Mylonitized graywacke with narrow biotite-rich zones forming mini-duplexes; cut by later, concordant quartz vein; quite annealed; local melting as in LB-19. |
| LB-25 | 6°33.0′N 1°25.6′W | Graywacke (?) | Localized melting perhaps as a result of shearing/friction? Similar to LB-19, but with more biotite; lots of melting in felsic bands; biotite to large extent oxidized. |
| LB-27 | 6°34.6′N 1°26.6′W | Quartzite | Most grains subaligned and elongated; minor annealing at grain margins; sutured texture; unshocked. |
| LB-28 | 6°34.6′N 1°26.6′W | Granite dike | Plagioclase-bearing, with large biotite porphyroblasts; rounded quartz and partially melted K-feldspar clasts; unshocked. |
| LB-35 | 6°33.1′N 1°22.6′W | Pepiakese granite | Two-mica granite, medium-grained; orthoclase and plagioclase are significantly sericitized; microcline is not; all quartz and some of the K-feldspar completely recrystallized; unshocked. |
| LB-36 | 6°33.1′N 1°22.6′W | Granite | Fine-grained biotite-granite, with some secondary muscovite (alteration after feldspar); displays slight gneissocity (biotite flakes are sub-aligned); biotite is altered as well, as shown, e.g., in reduced birefringence and pleochroism; unshocked. |
| LB-30 | 6°33.9′N 1°23.9′W | Impact glass | Clast from suevite (northern crater sector); highly vesiculated glass of variable color; locally cracks are filled with phyllosilicates (alteration product); very little devitrification; only oxidic remnants of mafic precursor minerals, such as biotite; some felsic mineral clasts are converted to diaplectic quartz glass or fused melt; some glass fragments with ballen structure. |
| LB-31A-E | 6°33.9′N 1°23.9′W | Impact glass | Clast from suevite; altered glass; contains a cm-size clast of partially melted graywacke; also a highly shocked clast of microgranite (K-feldspar and quartz), with every grain displaying PDFs. |
| LB-31A-F | 6°33.9′N 1°23.9′W | Impact glass | Clast from suevite; altered impact glass similar to LB-31A-E; contains diaplectic quartz glass fragments. |
| LB-31A-G | 6°33.9′N 1°23.9′W | Impact glass | Clast from suevite; devitrified and altered; clasts contain abundant PDFs and are, in part, diaplectic quartz glass. |
| LB-31A-H | 6°33.9′N 1°23.9′W | Impact glass | Clast from suevite; altered; contains some granitic clasts; a partially isotropized K-feldspar grain. |
| LB-30A | 6°33.9′N 1°23.9′W | Suevite | No thin section (from same rock of LB-30B). |
| LB-30B | 6°33.9′N 1°23.9′W | Suevite | Similar to LB-41; glass-rich; thin section dominated by impact glass; fluidal texture, highly porous (≈10 vol%), partially devitrified and oxidized; very few clasts, all completely annealed. |
| LB-41 | 6°33.9′N 1°23.9′W | Suevite | Contains a several cm large impact melt clast; mixed clast population of meta-sedimentary (greywacke, schist) and granitoid-derived fragments; numerous clasts identifiable by their texture only, because they are completely isotropized; matrix composed of finest-grained, microscopically unresolvable phyllosilicates. |
| BH1-0520 | 6°33.9′N 1°23.9′W | Suevite | Sample from drill hole BH1 at 5.2 m depth; altered, greenish gray in color with dark gray to greenish black, glassy inclusions and light-colored, granitic and mineral and metasediment clasts in a fine-grained clastic matrix; quartz clasts with lots of PDFs or ballen structure and, possibly, high pressure polymorphs, together with diaplectic glasses. |
| BH1-1300 | 6°33.9′N1° 23.9′W | Suevite | Sample from drill-hole BH1 at 13 m depth; quartz clasts with multiple sets of PDFs or composed of diaplectic glass. |
| BH3-0290 | 6°34.0′N 1°24.1′W | Suevite | Sample from drill-hole BH3 at 2.9 m depth; altered, greenish gray in color with abundant vesicular glass inclusions, as well as granitoid- and metasediment-derived clasts in a fine-grained clastic matrix; many clasts of diaplectic glass and often PDFs in quartz clasts. |
| BH3-0865 | 6°34.0′N 1°24.1′W | Suevite | Sample from BH3, at 8.65 m depth; greenish gray with inclusions of vesicular glass fragments and clasts of phyllite, graywacke, and granitoids in a fine-grained clastic matrix. |

Amphibolite samples AS1, AS1-2, AS2, and AS3 were taken about 40 km to the northeast of the Ashanti mine. They experienced a strong retrograde greenschist-facies overprint. Samples AS1, AS1-2, and AS2 are fine-grained massive metabasalts, which consist of actinolite, epidote, chlorite, albite (some with andesine cores), quartz, and carbonate. Accessories are ilmenite that is replaced by titanite, as well as zircon and apatite. Sample AS3 is less retrograded and contains quartz, plagioclase (25–44 mole% An), hornblende (tschermakite), biotite, and epidote. These samples do not contain sulfide mineralization.

Quartz-pebble conglomerate samples T and T-2 are from the Tarkwaian in Tarkwa Mine (e.g., Hirdes and Nunoo 1994). They have >90 vol% quartz pebbles. The matrix of both samples consists of fine- to medium-grained, xenoblastic quartz followed by black sand minerals like hematite, magnetite, and Fe,Ti oxides. Additional accessories are epidote, zircon, gold, tourmaline, albite, actinolite, chlorite, apatite, carbonate, sericite, and very rare pyrite. These samples contain less sulfides than the Ashanti mine samples.

## ANALYTICAL METHODS

### Major and Trace Element Analyses

Major elements were analyzed on powdered samples by standard X-ray fluorescence (XRF) procedures (for details on procedure, precision, and accuracy, see Reimold et al. 1994). The concentrations of V, Cu, Y, and Nb were also determined by XRF analysis. All other trace elements—Sc, Cr, Co, Ni, Zn, Ga, As, Br, Rb, Sr, Zr, Sb, Cs, Ba, rare earth elements, Hf, Ta, Th, and U—were determined on about 150 mg aliquots by instrumental neutron activation analysis (INAA) following procedures described by Koeberl (1993). The Na, K, Sr, and Zr data given are averages from XRF and INAA data.

### PGE, Au, Ag, and Re Analyses

The contents of the PGEs, Au, Ag, and Re were determined using an anion exchange preconcentration procedure with INAA and ultrasonic nebulization ICP-MS analysis. Anion exchange preconcentration has been widely applied to separate the PGEs from various geological samples (e.g., Crocket et al. 1968; Colodner et al. 1996; Jarvis et al. 1997; Yi and Masuda 1996). In previous studies (Dai et al. 2000), an α-amino pyridine resin preconcentration procedure was established, and the adsorption behavior of iridium on the resin was investigated. For the present study, an optimized anion exchange preconcentration procedure was developed. Sample dissolution was performed using an alkali fusion technique. Typically, about 1 g sample aliquot was mixed with 5 g sodium peroxide and fused at 650 °C for half an hour in a 50 ml high-purity pyrolytic graphic crucible. The fused cake was dissolved with concentrated HCl and transferred into a 50 ml PTFE beaker with deionized water. Then, the sample solution was evaporated to near dryness under an infrared lamp and taken up in 25 ml of 0.4 M HCl. The solution was centrifuged at 3500 rpm for 10 min., and the small amount of colloidal remnant (most likely aluminosilicic acid) was discarded after having been washed and centrifuged three times with about 8 ml of 0.4 M HCl. The supernatant was combined for chlorination. As the higher oxidation states of the PGEs are strongly adsorbed by anion resin and the lower oxidation species are bound less effectively (Crocket et al. 1968; Yi and Masuda 1996), it is necessary to convert the PGEs to their higher oxidation states before the addition of the sample solution to the anion exchange column. For this purpose, chlorine gas was vigorously percolated through the sample solution for 3 min. The solution was, then, sealed off and agitated occasionally for more than 12 hr to ensure optimal chlorination. Then, the sample was passed through an anion resin column (Dowex 1 × 8, 50–100 mesh, 20 mm long, and 7 mm diameter) at 2 ml/min. To avoid the possible loss of PGEs from this small column, the solution was re-introduced into the column for a second adsorption cycle. Then, the resin was rinsed with 10 ml of 1 M HCl, followed by washing with deionized water to neutralize the eluate.

After completion of this pre-concentration stage, the concentrations of PGEs, Au, Ag, and Re were measured by NAA and USN-ICP-MS, respectively. For neutron activation analysis, the resin was removed with deionized water from the column, filtered, and packed into a small quartz vial. After being heated at 200 °C for 6 hr, the vial was sealed for long-term (10 hr) irradiation at a thermal neutron flux of $6 \times 10^{13}$ n/cm$^{-2}$ • s$^{-1}$. Three counting cycles were carried out using a high purity germanium (HPGe) detector, after 4, 10, and 20 days of cooling time, respectively.

For USN-ICP-MS determination, a separate batch of the samples was pre-concentrated. After adsorption, the resin was transferred into a 10 ml quartz crucible and ashed at 550 °C for 4 hr. The ash was dissolved in 0.5 ml of concentrated HCl and evaporated to near-dryness. Then, the sample was dissolved in 0.5 ml of concentrated nitric acid, filtered, and washed with 2% $HNO_3$ solution into a 25 ml volumetric flask. After addition of internal In and Tl standards, the sample solution of about 3% $HNO_3$ acidity was analyzed by external calibration on a Perkin-Elmer/SCIEX Elan 5000A ICP-MS instrument. A CETAC U-5000AT Ultrasonic Nebulizer was used as an enhanced sample introduction system. The abundances of the $^{101}$Ru, $^{105}$Pd, $^{107}$Ag, $^{185}$Re, $^{189}$Os, $^{193}$Ir, $^{195}$Pt, and $^{197}$Au isotopes were analyzed. The WMG-1 and WITS-1 reference materials were analyzed in duplicate to determine accuracies and precisions for this procedure (Table 4).

For comparison, the Pt, Pd, Rh, Ir, and Au in several samples (aliquots of three suevites, LB-30A, LB-30B, and LB-41, one greywacke, LB-22, one phyllite, LB-37, and one granite, LB-36), as well as the set of samples from the Ashanti and Tarkwa mines, were analyzed by ICP-MS after Ni-sulfide fire assay with Te coprecipitation. All information regarding

the procedures for these analyses, as well as related precision and accuracy values, were given by Koeberl et al. (2000) and Huber et al. (2001).

## RESULTS AND DISCUSSSION

### Major and Trace Element Composition

The major and trace element compositions of Bosumtwi target rocks, dike samples, and impactites are given in Tables 2a and 2b. Average compositions, compositional ranges for the different lithological groups, and a comparison with data for target rocks and Ivory Coast tektites and microtektites from Koeberl et al. (1998) are listed in Table 3. Koeberl et al. (1998) reported chemical compositions for the following country rock types from Bosumtwi: shale, phyllite-greywacke, granite dikes, and Pepiakese granite. Here, compositions of greywacke, granites, schist, meta-sandstone, quartzite, the so-called "locally melted greywacke," suevites, and impact glass are added.

The major element compositions of impactites and the various target rocks show limited variation and agree with each other within the range displayed by these rock types (Fig. 2; Table 3). Compared to most target rocks, the impactites have somewhat higher CaO and L.O.I. values, which might be related to the presence of significant amounts of carbonate occurring as secondary vein and pore space fillings and alteration products of impact glass. In addition, it has been noted during our first analyses of suevite samples from the crater fill that carbonate-rich bands do occur quite frequently intercalated with other metasediments. The Harker variation diagrams (Fig. 2) indicate a trend between the target rocks and the impactites, especially in terms of $SiO_2$ contents; this is the likely result of the mixing relationship between these rocks. Sample LB-30, an impact glass clast with relatively low $SiO_2$ content (in comparison to the other impact glasses), has the highest abundances of the other elements determined in this study. Quartzite sample LB-27 has the highest $SiO_2$ content and, accordingly, is relatively depleted in all other elements. The major element contents of four impact glasses (except LB-30) agree well with the average composition of Ivory Coast tektites (see Koeberl et al. 1997). In terms of major and many trace elements, the granite dike LB-28 is compositionally very similar to the Pepiakese granite sample, but different compared to the locally melted greywacke samples (Tables 2a and 3). In contrast to the average phyllite, the quartz-rich phylite LB-17 has lower trace element contents, whereas another phyllite sample, LB-12, has a composition similar to that of granite (Tables 2a and 3).

As shown in Figs. 3a and 3b, the chondrite-normalized abundance patterns for the rare earth elements (REE) for all Bosumtwi target rocks and impactites are fairly similar. With the exception of shale, all other target rock types lack a distinct Eu anomaly. Total REE abundances are generally similar to Archean upper crust (according to Taylor and McLennan 1985). Very similar REE patterns are obtained for Bosumtwi suevites and impact glasses, as well as for Ivory Coast tektites and microtektites (Fig. 3b; also Koeberl et al. 1997). Bosumtwi target rocks cover a slightly wider range of REE abundances than the impactites and tektites (Fig. 3a).

Compared to Ivory Coast tektites and microtektites, the Bosumtwi impact glasses have a similar content of lithophile elements, a lower content of siderophile elements, and a higher content of volatile elements (Fig. 4). The relatively high abundance of volatile elements (e.g., Zn, As, Sb, and Cs) in impact glass can be explained by significant loss of these elements during the more complete melting of tektite-forming material (cf. Koeberl 1994). In comparison to suevite and impact glass from Bosumtwi, tektites and microtektites are characterized by somewhat higher Cr, Co, and Ni abundances. This implies a possibly larger meteoritic component in tektite material, but could also be caused by the chemical differences of the respective target rock mixtures, from which tektites and impact glasses were derived.

### PGEs, Au, Ag, and Re

Results for the platinum group elements (PGEs), Au, Ag, and Re, in Bosumtwi target rocks and impactites are given in Table 4. The data for Ir, Au, and Re are more precise with NAA, whereas Pt, Pd, and Ru are better determined by USN-ICP-MS. No Rh values are available from this latter technique, because significant loss of this element was observed during pre-treatment of samples (Dai et al. 2001). As noted above, several suevites and target rocks, as well as the ore mineralized samples from the mines in Obuasi, were also analyzed by ICP-MS after Ni-sulfide fire assay with Te co-precipitation (Table 5). As different samples were analyzed, it is not possible to directly compare respective results, but it seems that, in similar samples, slightly lower Ir values were obtained by the ICP-MS/fire assay method compared to the anion exchange method. It is also possible that the anion preconcentration data suffer from high Pt blanks, as discussed by Dai et al. (2001). We note that the anion exchange method has a lower analytical precision and accuracy compared to the NiS-ICP-MS method. Due to a limited overlap between the analyses, a detailed discussion of the advantages and disadvantages of the respective methods is beyond the scope of the present work.

The CI chondrite-normalized abundances of PGEs, Au, Ag, and Re for Bosumtwi target rocks and impactites are shown in Fig. 5a and related iron meteorite-normalized abundances are shown in Fig. 5b (see below). A normalization to type IIIAB iron meteorite type was chosen because a) this is a common iron meteorite type and most of the small impact craters produced by iron meteorite projectiles involved this type (cf. Koeberl 1998), b) iron

Table 2a. Major and trace element composition of target rocks and impactites from the Bosumtwi impact structure.

| | Schist | | Meta-sandstone | Graywacke | | Quartzite | Granite dike | Pepiakese granite | Locally melted graywacke | |
|---|---|---|---|---|---|---|---|---|---|---|
| | LB-6 | LB-7 | LB-8 | LB-12 | LB-17 | LB-27 | LB-28 | LB-35 | LB-19 | LB-21 |
| $SiO_2$ | 69.51 | 70.82 | 71.36 | 67.53 | 78.72 | 100.53 | 73.98 | 72.99 | 62.52 | 66.09 |
| $TiO_2$ | 0.39 | 0.55 | 0.56 | 0.65 | 0.39 | 0.14 | 0.20 | 0.31 | 0.81 | 0.69 |
| $Al_2O_3$ | 12.66 | 14.11 | 14.23 | 15.99 | 10.11 | <0.01 | 15.67 | 14.9 | 14.14 | 13.41 |
| $Fe_2O_3$ | 6.12 | 4.74 | 4.73 | 5.69 | 3.73 | 0.56 | 1.12 | 1.86 | 6.86 | 6.87 |
| MnO | 0.04 | 0.04 | 0.06 | 0.07 | 0.04 | 0.02 | 0.03 | 0.07 | 0.07 | 0.09 |
| MgO | 1.16 | 1.11 | 1.43 | 1.97 | 0.86 | <0.01 | 0.25 | 0.59 | 7.29 | 4.28 |
| CaO | 0.2 | 0.16 | 0.38 | 0.43 | 0.23 | 0.02 | 0.29 | 1.94 | 0.74 | 0.80 |
| $Na_2O$ | 1.47 | 2.95 | 3.61 | 2.86 | 2.92 | 0.0023 | 4.77 | 4.46 | 2.40 | 2.68 |
| $K_2O$ | 1.99 | 1.33 | 1.48 | 1.81 | 0.75 | 0.01 | 1.84 | 1.78 | 0.23 | 0.36 |
| $P_2O_5$ | 0.10 | 0.04 | 0.05 | 0.09 | 0.08 | 0.01 | 0.01 | 0.05 | 0.15 | 0.15 |
| L.O.I. | 6.52 | 3.86 | 1.97 | 3.19 | 1.9 | <0.01 | 1.97 | 1.29 | 5.30 | 4.27 |
| Total | 100.16 | 99.71 | 99.86 | 100.28 | 99.73 | 101.29 | 100.13 | 100.24 | 100.51 | 99.69 |
| Sc | 14.2 | 10.4 | 10.2 | 13.5 | 6.46 | 0.092 | 1.83 | 2.29 | 14.4 | 13 |
| V | 109 | 105 | 101 | 121 | 101 | <15 | <15 | 18 | 119 | 101 |
| Cr | 84.4 | 84.4 | 79.1 | 91 | 56.7 | 6 | 5.5 | 10.6 | 398 | 360 |
| Co | 9.74 | 8.87 | 10.5 | 14 | 5.94 | 0.88 | 6.38 | 2.38 | 24.4 | 18.2 |
| Ni | 65 | 23 | 42 | 21 | 43 | 2.5 | 8 | 26 | 270 | 191 |
| Cu | 19 | <2 | 8 | 16 | <2 | <2 | <2 | <2 | <2 | <2 |
| Zn | 55.5 | 61.2 | 59.9 | 70.4 | 37.5 | 0.76 | 16.8 | 48 | 84.2 | 103 |
| Ga | 11 | 7.9 | 1.9 | 5.9 | 4.8 | 0.8 | 5.5 | 11.5 | 0.13 | 9.1 |
| As | 1.81 | <2.1 | <2.1 | <2.3 | 0.14 | 0.59 | 0.78 | 1.4 | 2.1 | 1.7 |
| Br | 1.6 | 0.1 | 0.55 | <1.8 | <1.6 | 0.3 | 0.57 | 0.02 | 0.62 | 0.62 |
| Rb | 15.6 | 49.2 | 48.2 | 69.4 | 34.8 | <2.2 | 51 | 68 | 6.55 | 28.8 |
| Sr | 140 | 346 | 345 | 302 | 238 | 1.6 | 392 | 377 | 203 | 239 |
| Y | 43 | 13 | 12 | 9 | 12 | <3 | <3 | 4 | 10 | 13 |
| Zr | 114 | 130 | 148 | 98 | 100 | 1.1 | 52 | 113 | 90 | 120 |
| Nb | 7 | 8 | 8 | 8 | 8 | 6 | 6 | 7 | 7 | 9 |
| Sb | 0.15 | 0.12 | 0.1 | 0.13 | 0.07 | 0.04 | 0.11 | 0.16 | 0.11 | 0.08 |
| Cs | 1.36 | 2.39 | 2.38 | 2.82 | 2.17 | 0.043 | 1.67 | 3.19 | 0.78 | 1.34 |
| Ba | 901 | 425 | 612 | 644 | 374 | <11 | 652 | 583 | 136 | 192 |
| La | 32.2 | 19.7 | 24.6 | 16.4 | 17.4 | 0.13 | 12.8 | 25.8 | 11.8 | 6.53 |
| Ce | 66 | 30.6 | 36.4 | 32.4 | 33.4 | 0.34 | 29.2 | 50.4 | 17.8 | 9.95 |
| Nd | 32 | 20 | 21 | 17 | 15 | <0.4 | 11 | 24 | 12 | 7 |
| Sm | 6.24 | 3.41 | 4.33 | 3.26 | 2.39 | 0.025 | 1.78 | 3.61 | 2.81 | 1.83 |
| Eu | 1.96 | 1.06 | 1.32 | 0.97 | 0.7 | 0.012 | 0.51 | 1.07 | 0.94 | 0.7 |
| Gd | 5.4 | 2.8 | 3.7 | 3 | 1.8 | 0.04 | 1.3 | 1.8 | 2.8 | 1.9 |
| Tb | 0.92 | 0.42 | 0.57 | 0.48 | 0.3 | <0.02 | 0.18 | 0.25 | 0.45 | 0.33 |
| Tm | 0.44 | 0.18 | 0.24 | 0.22 | 0.16 | 0.008 | 0.045 | 0.06 | 0.16 | 0.19 |
| Yb | 3.15 | 1.21 | 1.6 | 1.56 | 1.18 | 0.03 | 0.24 | 0.39 | 1.05 | 1.36 |
| Lu | 0.46 | 0.18 | 0.24 | 0.26 | 0.18 | 0.004 | 0.025 | 0.062 | 0.16 | 0.22 |
| Hf | 1.32 | 3.55 | 3.5 | 2.99 | 3.24 | 0.024 | 1.44 | 2.66 | 3.2 | 2.74 |
| Ta | 0.09 | 0.34 | 0.24 | 0.4 | 0.21 | 0.02 | 0.11 | 0.21 | 0.31 | 0.23 |
| Ir (ppb) | 1 | 1.8 | 2.1 | <2.3 | 1.5 | 0.14 | <1.1 | 2.8 | <2.4 | 1.4 |
| Au (ppb) | 8.2 | 4.2 | 5.7 | <4.6 | 2.9 | 1.2 | 0.8 | 8.2 | <4.5 | 4.8 |
| Th | 2.27 | 3 | 3.14 | 3.08 | 2.55 | 0.004 | 2.13 | 2.51 | 2.08 | 2.38 |
| U | 2.11 | 0.48 | 0.58 | 0.38 | 0.39 | 0.08 | 0.32 | 0.7 | 0.36 | 0.86 |
| K/U | 7829 | 23,002 | 21,183 | 39,541 | 15,964 | 1038 | 47,734 | 21,110 | 5304 | 3475 |
| Th/U | 1.08 | 6.25 | 5.41 | 8.11 | 6.54 | 0.05 | 6.66 | 3.59 | 5.78 | 2.77 |
| La/Th | 14.2 | 6.57 | 7.83 | 5.32 | 6.82 | 30 | 6.01 | 10.3 | 5.67 | 2.74 |
| Zr/Hf | 86.4 | 36.6 | 42.3 | 32.8 | 30.9 | 45.8 | 36.1 | 42.5 | 28.1 | 43.8 |
| Hf/Ta | 14.7 | 10.4 | 14.6 | 7.48 | 15.4 | 1.2 | 13.1 | 12.7 | 10.3 | 11.9 |
| $La_N/Yb_N$ | 6.73 | 10.7 | 10.2 | 6.93 | 9.68 | 7.18 | 35.1 | 43.6 | 7.40 | 3.17 |
| Eu/Eu* | 1.00 | 1.01 | 0.98 | 0.93 | 0.98 | 1.15 | 0.97 | 1.13 | 1.01 | 1.13 |

Major element data in wt%; trace element data in ppm, except as noted. All Fe as $Fe_2O_3$. Blank spaces: not determined.

Table 2a. *Continued.* Major and trace element composition of target rocks and impactites from the Bosumtwi impact structure.

| | Locally melted graywacke *(continued)* | Suevite | | | | Impact glass | | | | |
|---|---|---|---|---|---|---|---|---|---|---|
| | LB-25 | BH1/0520 | BH1/1300 | BH3/0290 | BH3/0865 | LB-30 | LB-31A-E | LB-31A-F | LB-31A-G | LB-31A-H |
| $SiO_2$ | 65.30 | 64.74 | 64.44 | 64.06 | 63.17 | 58.17 | 64.54 | 64.86 | 64.94 | 64.11 |
| $TiO_2$ | 0.78 | 0.61 | 0.67 | 0.67 | 0.62 | 0.83 | 0.60 | 0.62 | 0.62 | 0.62 |
| $Al_2O_3$ | 14.32 | 16.20 | 16.15 | 15.84 | 14.64 | 20.25 | 16.02 | 15.59 | 15.95 | 15.50 |
| $Fe_2O_3$ | 6.52 | 5.99 | 5.59 | 5.85 | 6.88 | 7.78 | 5.03 | 5.06 | 4.67 | 5.23 |
| MnO | 0.13 | 0.08 | 0.14 | 0.06 | 0.19 | 0.07 | 0.04 | 0.04 | 0.05 | 0.04 |
| MgO | 3.69 | 1.87 | 1.63 | 0.95 | 1.27 | 1.82 | 0.79 | 0.70 | 0.73 | 0.75 |
| CaO | 0.21 | 1.87 | 2.24 | 1.84 | 1.19 | 0.86 | 1.25 | 1.48 | 1.35 | 1.20 |
| $Na_2O$ | 1.74 | 2.28 | 2.12 | 1.91 | 1.62 | 2.20 | 2.18 | 2.30 | 2.38 | 2.48 |
| $K_2O$ | 1.57 | 1.89 | 1.6 | 1.15 | 0.97 | 2.55 | 1.57 | 1.79 | 1.74 | 1.59 |
| $P_2O_5$ | 0.13 | 0.11 | 0.12 | 0.09 | 0.08 | 0.07 | 0.08 | 0.10 | 0.09 | 0.07 |
| L.O.I. | 5.24 | 4.86 | 5.76 | 7.12 | 9.21 | 5.99 | 7.07 | 7.12 | 7.56 | 8.19 |
| Total | 99.63 | 100.51 | 100.48 | 99.54 | 99.84 | 100.59 | 99.17 | 99.66 | 100.08 | 99.78 |
| Sc | 14.5 | 13.7 | 13.8 | 14.9 | 14.3 | 19.3 | 13.9 | 14.2 | 14.1 | 15.3 |
| V | 127 | 106 | 98 | 96 | 118 | 145 | 96 | 89 | 90 | 90 |
| Cr | 360 | 175 | 213 | 210 | 181 | 190 | 121 | 125 | 115 | 116 |
| Co | 24.6 | 18.4 | 14.6 | 15.6 | 19.8 | 24 | 22.7 | 21.1 | 20.7 | 22.4 |
| Ni | 195 | 64 | 65 | 71 | 79 | 73 | 56 | 71 | 81 | 70 |
| Cu | <2 | 17 | 17 | 19 | 22 | 15 | 33 | 32 | 30 | 32 |
| Zn | 89.4 | 76 | 61 | 69 | 76 | 128 | 83.5 | 89.6 | 79 | 88.6 |
| Ga | 11.2 | | | | | 21 | 13.4 | 17.1 | 17.1 | 5.8 |
| As | 19.8 | 4.8 | 2.9 | 2.7 | 2.3 | 5.1 | 4.6 | 4.6 | 4.2 | 0.66 |
| Br | 0.56 | 0.23 | 0.21 | 0.16 | 0.18 | <1.3 | 0.42 | <1.2 | 0.59 | <1.2 |
| Rb | 61.5 | 71.2 | 64.3 | 43.5 | 45.1 | 100 | 94 | 78 | 71.8 | 72 |
| Sr | 239 | 338 | 330 | 327 | 297 | 260 | 320 | 305 | 308 | 297 |
| Y | <3 | 19 | 15 | 15 | 15 | 19 | 15 | 17 | 14 | 17 |
| Zr | 113 | 128 | 131 | 136 | 121 | 152 | 161 | 163 | 153 | 135 |
| Nb | 9 | 8 | 9 | 9 | 8 | 11 | 9 | 10 | 9 | 9 |
| Sb | 0.08 | 0.33 | 0.34 | 0.44 | 0.42 | 0.2 | 0.31 | 0.45 | 0.34 | 0.18 |
| Cs | 2.49 | 3.39 | 2.81 | 2.77 | 2.51 | 5.01 | 3.95 | 4.12 | 4 | 3.59 |
| Ba | 424 | 684 | 541 | 617 | 521 | 986 | 610 | 705 | 573 | 603 |
| La | 15.8 | 22.0 | 18.8 | 20.8 | 16.7 | 27.9 | 29.5 | 33.7 | 30.2 | 38.2 |
| Ce | 33.8 | 42.3 | 41.4 | 45.8 | 36.0 | 45.7 | 44.1 | 51.6 | 50.6 | 57.9 |
| Nd | 13 | 23 | 17 | 20 | 15 | 27 | 24 | 26 | 29 | 26 |
| Sm | 3.29 | 4.55 | 3.67 | 3.53 | 3.1 | 4.26 | 4.44 | 5.32 | 4.57 | 5.62 |
| Eu | 1.04 | 1.3 | 1.1 | 1.27 | 1.02 | 1.38 | 1.18 | 1.34 | 1.2 | 1.52 |
| Gd | 3 | 3.72 | 3.43 | 3.09 | 3.32 | 3.1 | 3.3 | 4.4 | 3.1 | 3.8 |
| Tb | 0.46 | 0.67 | 0.45 | 0.47 | 0.44 | 0.56 | 0.55 | 0.69 | 0.5 | 0.65 |
| Tm | 0.17 | 0.26 | 0.23 | 0.2 | 0.31 | 0.27 | 0.21 | 0.23 | 0.2 | 0.24 |
| Yb | 1.11 | 1.92 | 1.44 | 1.35 | 1.35 | 1.96 | 1.3 | 1.56 | 1.3 | 1.46 |
| Lu | 0.17 | 0.24 | 0.2 | 0.22 | 0.21 | 0.3 | 0.17 | 0.23 | 0.19 | 0.22 |
| Hf | 2.88 | 3.61 | 3.4 | 3.42 | 2.85 | 3.97 | 3.17 | 4.02 | 3.46 | 3.7 |
| Ta | 0.27 | 0.35 | 0.3 | 0.31 | 0.3 | 0.55 | 0.38 | 0.38 | 0.38 | 0.31 |
| Ir (ppb) | <2.3 | 0.91 | <2.6 | <3 | <2.9 | <2.6 | 1.2 | 1.3 | 0.4 | 0.9 |
| Au (ppb) | 3.4 | 5.8 | 39.9 | 4.7 | 2.2 | 3.6 | 3.9 | 14 | 9.3 | 7.5 |
| Th | 2.07 | 3.28 | 3.44 | 3.37 | 2.94 | 3.92 | 3.32 | 3.63 | 3.36 | 3.52 |
| U | 0.69 | 0.84 | 1.43 | 1.23 | 0.84 | 0.75 | 0.91 | 0.73 | 0.99 | 0.65 |
| K/U | 18,889 | 15,683 | 13,277 | 9543 | 8049 | 28,225 | 14,322 | 20,356 | 14,591 | 20,307 |
| Th/U | 3.00 | 3.90 | 2.41 | 2.74 | 3.50 | 5.23 | 3.65 | 4.97 | 3.39 | 5.42 |
| La/Th | 7.63 | 6.71 | 5.46 | 6.17 | 5.68 | 7.12 | 8.89 | 9.28 | 8.99 | 10.9 |
| Zr/Hf | 39.2 | 35.5 | 38.5 | 39.8 | 42.5 | 38.3 | 50.8 | 40.5 | 44.2 | 36.5 |
| Hf/Ta | 10.7 | 10.3 | 11.3 | 11.0 | 9.50 | 7.22 | 8.34 | 10.6 | 9.11 | 11.9 |
| $La_N/Yb_N$ | 9.37 | 7.74 | 8.82 | 10.41 | 8.36 | 9.37 | 15.0 | 14.2 | 15.3 | 17.2 |
| Eu/Eu* | 0.99 | 0.97 | 0.95 | 1.18 | 0.97 | 1.10 | 0.90 | 0.82 | 0.92 | 0.94 |

Major element data in wt%; trace element data in ppm, except as noted. All Fe as $Fe_2O_3$. Blank spaces: not determined.

Table 2b. Major and trace element composition of Bosumtwi rocks (XRF data).

| | Graywacke | Phyllite | Granite | Suevite | | |
|---|---|---|---|---|---|---|
| | LB-22 | LB-37 | LB-36 | LB-30a | LB-30b | LB-41 |
| $SiO_2$ | 67.31 | 59.35 | 66.36 | 63.30 | 53.12 | 63.01 |
| $TiO_2$ | 0.59 | 0.81 | 0.67 | 0.66 | 0.79 | 0.66 |
| $Al_2O_3$ | 15.63 | 17.97 | 16.93 | 15.40 | 21.13 | 17.23 |
| $Fe_2O_3$ | 5.89 | 10.50 | 4.81 | 6.37 | 9.71 | 5.91 |
| MnO | 0.03 | 0.13 | 0.05 | 0.05 | 0.06 | 0.04 |
| MgO | 1.87 | 0.44 | 1.74 | 0.79 | 2.02 | 0.91 |
| CaO | 0.88 | 0.00 | 1.09 | 1.17 | 1.06 | 0.90 |
| $Na_2O$ | 2.60 | 1.84 | 3.90 | 1.64 | 1.48 | 1.81 |
| $K_2O$ | 1.72 | 2.48 | 1.63 | 1.35 | 3.10 | 1.11 |
| $P_2O_5$ | 0.09 | 0.12 | 0.24 | 0.06 | 0.10 | 0.06 |
| L.O.I. | 3.41 | 5.33 | 3.25 | 8.75 | 6.63 | 8.18 |
| Total | 100.03 | 98.97 | 100.67 | 99.56 | 99.20 | 99.81 |
| V | 111 | 131 | 64 | 92 | 150 | 110 |
| Cr | 113 | 131 | 50 | 224 | 240 | 166 |
| Co | 16 | 30 | 12 | 23 | 28 | 24 |
| Ni | 38 | 60 | 13 | 69 | 100 | 61 |
| Cu | 13 | 43 | <2 | 32 | 29 | 27 |
| Zn | 59 | 136 | 53 | 78 | 129 | 85 |
| Rb | 60 | 90 | 59 | 43 | 121 | 36 |
| Sr | 327 | 194 | 361 | 277 | 300 | 252 |
| Y | 11 | 22 | 18 | 9 | 29 | 12 |
| Zr | 116 | 164 | 131 | 131 | 156 | 136 |
| Nb | 9 | 12 | 9 | 10 | 11 | 10 |
| Ba | 661 | 639 | 676 | 605 | 947 | 506 |

Major element data in wt%; trace element data in ppm. All measurements by XRF. All Fe as $Fe_2O_3$.

meteorites show such large variations in siderophile element abundances that a reasonably constrained average cannot be calculated, and c) for this meteorite type an internally consistent data set was available for comparison.

On first glance, the elevated Ru, Pd, Os, Ir, and Ag contents in impact glasses suggest the presence of a meteoritic contribution. However, the target rocks also have rather high PGE abundances, so that a significant difference between the abundances of these two groups of samples is not established (Table 4). High and variable Au and Pt abundances are noted in both target rocks and impactites, but, as mentioned before, we can not completely exclude that some high values for Pt and Au result from contamination. The relatively high values of regionally occurring lithologies could very well result from the fact that the Bosumtwi crater is located in an area known for its widespread gold mineralization (see below), as already recognized by Jones (1985) and Koeberl and Shirey (1993). Highly variable and high Au contents were also determined by a number of earlier workers in Bosumtwi target rocks (Jones 1985; Koeberl et al. 1998) and Ivory Coast tektites (Koeberl et al. 1997). The highest Ir value (3.7 ppb), accompanied by very high Pt and Au values (39 and 12.4 ppb, respectively), was obtained for Pepiakese granite sample LB-35. Taken at face value, 3.7 ppb Ir represent about 0.7% of a chondritic component, assuming a chondritic Ir content of about 500 ppb. On the other hand, a chondrite has about 500 ppm Co, 3200 ppm Cr, and 1.4 wt% Ni (see Koeberl 1998 for a discussion of average meteorite data); thus, 0.7% of a chondritic component contributes 3.5 ppm Co, 22.4 ppm Cr, and 98 ppm Ni. The Pepiakese granite sample LB-35 has 2.4 ppm Co, 10.6 ppm Cr, and 26 ppm Ni. This does not support the presence of 0.7% of a chondritic component. These values are on the low side compared to the schist, graywacke, and even sandstone, and lower than in the suevites and impact glass.

In contrast to the graywacke, schist, granite, and meta-sandstone samples, the so-called locally melted graywacke samples show somewhat higher Cr, Co, and Ni abundances (Table 3), but with regard to PGE abundances (Table 4), no apparent difference is observed for these sample groups.

A comparison of the indigenous abundances of PGE in the target rocks with PGE abundances in impactite samples (Table 4) does not allow to unambiguously identify a meteoritic component in the impact breccias (Fig. 6). In contrast, interesting observations can be derived from analysis of PGE interelement ratios (Fig. 7). In a plot of Pd/Ru versus Os/Ir, the impactites can be easily distinguished from the target rocks; all analyzed target rocks have significantly higher Pd/Ru and lower Os/Ir ratios than the impact glasses and suevites. The locally melted graywacke samples have also much lower Pd/Ru and higher Os/Ir ratios than the regionally occurring lithologies—values that are very close to CI chondrite values.

Siderophile element anomalies in impactites can be

Table 3. Average and range of compositions of target rocks and impactites from the Bosumtwi impact structure compared to Ivory Coast tektites and microtektites.

| | Schist | Shale | Graywacke-phyllite | Granite dike | Pepiakese granite | Locally melted graywacke | |
|---|---|---|---|---|---|---|---|
| | Average | Average | Average | Average | Average | Average | Range |
| $SiO_2$ | 70.17 ± 0.65 | 55.56 | 66.75 | 68.74 | 57.81 | 64.64 ± 1.41 | 62.52–66.09 |
| $TiO_2$ | 0.47 ± 0.08 | 0.84 | 0.66 | 0.50 | 0.46 | 0.76 ± 0.05 | 0.69–0.81 |
| $Al_2O_3$ | 13.39 ± 0.73 | 19.56 | 15.27 | 15.91 | 16.45 | 13.96 ± 0.36 | 13.41–14.32 |
| $Fe_2O_3$ | 5.43 ± 0.69 | 8.54 | 6.37 | 3.97 | 6.09 | 6.75 ± 0.15 | 6.52–6.87 |
| MnO | 0.04 ± 0.00 | 0.046 | 0.028 | 0.014 | 0.067 | 0.1 ± 0.02 | 0.07–0.13 |
| MgO | 1.14 ± 0.02 | 2.90 | 2.12 | 1.44 | 6.63 | 5.09 ± 1.47 | 3.69–7.29 |
| CaO | 0.18 ± 0.02 | 0.09 | 0.19 | 0.31 | 4.36 | 0.58 ± 0.25 | 0.21–0.8 |
| $Na_2O$ | 2.21 ± 0.74 | 1.00 | 2.26 | 4.14 | 6.04 | 2.27 ± 0.36 | 1.74–2.68 |
| $K_2O$ | 1.66 ± 0.33 | 2.89 | 1.80 | 1.92 | 0.67 | 0.72 ± 0.57 | 0.23–1.57 |
| $P_2O_5$ | 0.07 ± 0.03 | 0.08 | 0.06 | 0.06 | 0.10 | 0.14 ± 0.01 | 0.13–0.15 |
| L.O.I. | 5.19 ± 1.33 | 7.91 | 4.25 | 2.98 | 1.48 | 4.94 ± 0.44 | 4.27–5.3 |
| Total | 99.94 ± 0.23 | 99.41 | 99.76 | 99.98 | 100.15 | 99.94 ± 0.38 | 99.63–100.51 |
| Sc | 12.3 ± 1.9 | 23.4 | 15.5 | 9.76 | 17.5 | 14.0 ± 0.6 | 13–14.5 |
| V | 107 ± 2 | 184 | 134 | 91 | 110 | 116 ± 10 | 101–127 |
| Cr | 84.4 | 194 | 165 | 127 | 517 | 373 ± 17 | 360–398 |
| Co | 9.31 ± 0.44 | 22.6 | 12.1 | 9.66 | 30.4 | 22.4 ± 2.8 | 18.2–24.6 |
| Ni | 44 ± 21 | 79 | 48 | 49 | 172 | 219 ± 34 | 191–270 |
| Cu | 19 | 52 | 15.5 | 10.7 | 24.3 | <2 | <2 |
| Zn | 58.4 ± 2.8 | 143 | 104 | 82 | 90 | 92.2 ± 7.2 | 84.2–103 |
| Ga | 9.4 ± 1.6 | 24 | 67 | 37 | 73 | 6.8 4 ± 4 | 0.13–11.2 |
| As | 1.81 | 8.61 | 7.00 | 14.9 | 12.7 | 7.9 ± 8.0 | 1.7–19.8 |
| Br | 0.85 ± 0.75 | 0.23 | 0.18 | 0.15 | 0.16 | 0.6 ± 0.03 | 0.56–0.62 |
| Rb | 32.4 ± 16.8 | 104 | 65.2 | 69.9 | 22.4 | 32.3 ± 19.5 | 6.55–61.5 |
| Sr | 243 ± 103 | 118 | 152 | 342 | 377 | 227 ± 16 | 203–239 |
| Y | 28 ± 15 | 23.8 | 19 | 11 | 11 | 12 ± 2 | <3–13 |
| Zr | 122 ± 8 | 153 | 143 | 129 | 82 | 108 ± 12 | 90–120 |
| Nb | 7.5 ± 0.5 | 6.1 | 5.7 | 3.7 | 1.8 | 8 ± 1 | 7–9 |
| Sb | 0.14 ± 0.02 | 0.38 | 0.20 | 0.18 | 0.42 | 0.09 ± 0.01 | 0.08–0.11 |
| Cs | 1.88 ± 0.52 | 5.57 | 3.27 | 4.22 | 0.87 | 1.54 ± 0.64 | 0.78–2.49 |
| Ba | 663 ± 238 | 765 | 454 | 605 | 226 | 251 ± 116 | 136–424 |
| La | 26.0 ± 6.2 | 30.9 | 23.4 | 18.8 | 15.6 | 11.4 ± 3.2 | 6.53–15.8 |
| Ce | 48.3 ± 17.7 | 38.4 | 34.8 | 39.4 | 32.0 | 20.5 ± 8.9 | 9.95–33.8 |
| Nd | 26.0 ± 6.0 | 28.2 | 26.5 | 19.8 | 17.5 | 11 ± 2 | 7–13 |
| Sm | 4.83 ± 1.42 | 5.48 | 5.06 | 3.74 | 3.58 | 2.64 ± 0.54 | 1.83–3.29 |
| Eu | 1.51 ± 0.45 | 1.37 | 1.29 | 1.03 | 1.19 | 0.89 ± 0.13 | 0.7–1.04 |
| Gd | 4.1 ± 1.3 | 6.55 | 4.80 | 3.40 | 3.07 | 2.57 ± 0.44 | 1.9–3 |
| Tb | 0.67 ± 0.25 | 1.06 | 0.73 | 0.59 | 0.47 | 0.41 ± 0.06 | 0.33–0.46 |
| Tm | 0.31 ± 0.13 | 0.47 | 0.35 | 0.22 | 0.20 | 0.17 ± 0.01 | 0.16–0.19 |
| Yb | 2.18 ± 0.97 | 2.70 | 2.14 | 1.13 | 1.18 | 1.17 ± 0.12 | 1.05–1.36 |
| Lu | 0.32 ± 0.14 | 0.38 | 0.29 | 0.16 | 0.14 | 0.18 ± 0.02 | 0.16–0.22 |
| Hf | 2.44 ± 1.12 | 4.12 | 4.04 | 3.66 | 1.88 | 2.94 ± 0.17 | 2.74–3.2 |
| Ta | 0.22 ± 0.13 | 0.53 | 0.42 | 0.28 | 0.19 | 0.27 ± 0.03 | 0.23–0.31 |
| Ir (ppb) | 1.4 ± 0.4 | | | | | 0.42 ± 0.05 | 0.35–0.50 |
| Au (ppb) | 6.2 ± 2.0 | 11.8 | 10.3 | 21.5 | 18.3 | 5.2 ± 2.0 | 3.2–8.2 |
| Th | 2.64 ± 0.37 | 4.36 | 3.94 | 3.10 | 2.21 | 2.18 ± 0.14 | 2.07–2.38 |
| U | 1.30 ± 0.82 | 1.69 | 1.35 | 1.75 | 0.74 | 0.64 ± 0.18 | 0.36–0.86 |
| K/U | 15,416 ± 7586 | 14,406 | 11,389 | 9245 | 10,800 | 9222 ± 6444 | 3475–18,889 |
| Th/U | 3.67 ± 2.59 | 2.60 | 35.5 | 1.79 | 2.67 | 3.85 ± 1.29 | 2.77–5.78 |
| La/Th | 10.39 ± 3.82 | 7.10 | 6.15 | 6.00 | 10.9 | 5.35 ± 1.74 | 2.74–7.63 |
| Zr/Hf | 61.5 ± 24.9 | 37.1 | 10.11 | 35.4 | 51.9 | 37.03 ± 5.96 | 28.1–43.8 |
| Hf/Ta | 12.56 ± 2.12 | 8.28 | 2.95 | 14.55 | 12.71 | 10.97 ± 0.63 | 10.32–11.91 |
| $La_N/Yb_N$ | 8.72 ± 1.99 | 7.75 | 7.30 | 11.21 | 13.72 | 6.65 ± 2.32 | 3.17–9.37 |
| Eu/Eu* | 1.01 ± 0.01 | 0.73 | 0.83 | 0.88 | 1.16 | 1.04 ± 0.06 | 0.99–1.13 |

Major element data in wt%; trace element data in ppm, except as noted. All Fe as $Fe_2O_3$. Blank space: no data available.

[a]From Koeberl et al. (1998).

[b]From Koeberl et al. (1997).

Table 3. *Continued.* Average and range of compositions of target rocks and impactites from the Bosumtwi impact structure, compared to Ivory Coast tektites and microtektites.

| | Suevite | | Impact glass | | Ivory Coast | |
|---|---|---|---|---|---|---|
| | | | | | Tektite | Microtektite |
| | Average | Range | Average | Range | Average | Average |
| $SiO_2$ | 64.10 ± 0.49 | 63.17–64.74 | 63.32 ± 2.06 | 58.17–64.94 | 67.58 | 67.37 |
| $TiO_2$ | 0.64 ± 0.03 | 0.61–0.67 | 0.66 ± 0.07 | 0.6–0.83 | 0.56 | 0.59 |
| $Al_2O_3$ | 15.71 ± 0.53 | 14.64–16.20 | 16.66 ± 1.44 | 15.5–20.25 | 16.74 | 17.07 |
| $Fe_2O_3$ | 6.08 ± 0.40 | 5.59–6.88 | 5.55 ± 0.89 | 4.67–7.78 | 6.16 | 6.40 |
| MnO | 0.12 ± 0.05 | 0.06–0.19 | 0.05 ± 0.01 | 0.04–0.07 | 0.06 | 0.07 |
| MgO | 1.43 ± 0.32 | 0.95–1.87 | 0.96 ± 0.34 | 0.7–1.82 | 3.46 | 3.70 |
| CaO | 1.79 ± 0.30 | 1.19–2.24 | 1.23 ± 0.16 | 0.86–1.48 | 1.38 | 1.22 |
| $Na_2O$ | 1.98 ± 0.22 | 1.62–2.28 | 2.31 ± 0.1 | 2.18–2.48 | 1.90 | 1.63 |
| $K_2O$ | 1.40 ± 0.34 | 0.97–1.89 | 1.85 ± 0.28 | 1.57–2.55 | 1.95 | 1.86 |
| $P_2O_5$ | 0.10 ± 0.02 | 0.08–0.12 | 0.08 ± 0.01 | 0.07–0.1 | | |
| L.O.I. | 6.74 ± 1.43 | 4.86–9.21 | 7.19 ± 0.55 | 5.99–8.19 | 0.002 | |
| Total | 100.09 ± 0.40 | 99.54–100.51 | 99.86 ± 0.38 | 99.17–100.59 | 99.79 | 99.89 |
| Sc | 14.2 ± 0.4 | 13.7–14.9 | 15.4 ± 1.6 | 13.9–19.3 | 14.7 | 17.9 |
| V | 104 | 96–118 | 102 ± 17 | 89–145 | | |
| Cr | 195 ± 17 | 175–213 | 133 ± 23 | 115–190 | 244 | 292 |
| Co | 17.1 ± 2.0 | 14.6–19.8 | 22.2 ± 1.0 | 20.7–24 | 26.7 | 32.7 |
| Ni | 70 ± 5 | 64–79 | 70 ± 6 | 56–81 | 157 | 224 |
| Cu | 19 | 17–22 | 28 ± 5 | 15–33 | | |
| Zn | 70.5 ± 5.5 | 61–76 | 93.7 ± 13.7 | 79–128 | 23 | 12 |
| Ga | | | 14.9 ± 4.2 | 5.8–21 | 21 | 17 |
| As | 3.2 ± 0.8 | 2.3–4.8 | 3.8 ± 1.3 | 0.66–5.1 | 0.45 | 0.42 |
| Br | 0.20 ± 0.03 | 0.16–0.23 | 0.53 ± 0.07 | 0.42–<1.3 | 0.79 | 0.4 |
| Rb | 56.0 ± 11.7 | 43.5–71.2 | 83.2 ± 11.1 | 71.8–100 | 66 | 66.7 |
| Sr | 323 ± 13 | 297–338 | 298 ± 16 | 260–320 | 260 | 325 |
| Y | 16.0 ± 1.5 | 15–19 | 16 ± 2 | 14–19 | | |
| Zr | 129 ± 0 4.5 | 121–136 | 153 ± 7 | 135–163 | 134 | 215 |
| Nb | 8.5 ± 0.5 | 8–9 | 9.6 ± 0.7 | 9–11 | | |
| Sb | 0.38 ± 0.05 | 0.33–0.44 | 0.3 ± 0.08 | 0.18–0.45 | 0.23 | 0.21 |
| Cs | 2.87 ± 0.26 | 2.51–3.39 | 4.13 ± 0.35 | 3.59–5.01 | 3.67 | 3.2 |
| Ba | 591 ± 60 | 521–684 | 695 ± 120 | 573–986 | 327 | 620 |
| La | 19.6 ± 1.8 | 16.70–22.00 | 31.9 ± 3.2 | 27.9–38.2 | 20.7 | 25.9 |
| Ce | 41.4 ± 2.7 | 36.00–45.80 | 50.0 ± 4.1 | 44.1–57.9 | 41.9 | 55.1 |
| Nd | 18.8 ± 2.8 | 15–23 | 26 ± 1.3 | 24–29 | 21.8 | 27.3 |
| Sm | 3.71 ± 0.42 | 3.10–4.55 | 4.84 ± 0.5 | 4.26–5.62 | 3.95 | 5.10 |
| Eu | 1.17 ± 0.11 | 1.02–1.30 | 1.32 ± 0.11 | 1.18–1.52 | 1.2 | 1.43 |
| Gd | 3.39 ± 0.19 | 3.1–3.7 | 3.54 ± 0.45 | 3.1–4.4 | 3.43 | 4.40 |
| Tb | 0.51 ± 0.08 | 0.44–0.67 | 0.59 ± 0.06 | 0.5–0.69 | 0.56 | 0.74 |
| Tm | 0.25 ± 0.04 | 0.20–0.31 | 0.23 ± 0.02 | 0.2–0.27 | 0.30 | 0.31 |
| Yb | 1.52 ± 0.20 | 1.35–1.92 | 1.52 ± 0.2 | 1.3–1.96 | 1.79 | 2.07 |
| Lu | 0.22 ± 0.01 | 0.20–0.24 | 0.22 ± 0.03 | 0.17–0.3 | 0.24 | 0.31 |
| Hf | 3.32 ± 0.24 | 2.85–3.61 | 3.66 ± 0.28 | 3.17–4.02 | 3.38 | 4.28 |
| Ta | 0.32 ± 0.02 | 0.30–0.35 | 0.4 ± 0.06 | 0.31–0.55 | 0.34 | 0.42 |
| Ir (ppb) | 0.91 | 0.91 | 0.80 ± 0.27 | 0.42–1.12 | 0.4 | 0.9 |
| Au (ppb) | 13.2 ± 13.4 | 2.2–39.9 | 13.3 ± 8.9 | 4.1–27.4 | 41 | 0.8 |
| Th | 3.26 ± 0.16 | 2.94–3.44 | 3.55 ± 0.18 | 3.32–3.92 | 3.54 | 3.99 |
| U | 1.09 ± 0.25 | 0.84–1.43 | 0.81 ± 0.12 | 0.65–0.99 | 0.94 | 0.64 |
| K/U | 11,638 ± 2842 | 8049–15,683 | 19,560 ± 4082 | 14,322–28,225 | 17,287 | 21,343 |
| Th/U | 3.14 ± 0.56 | 2.41–3.90 | 4.53 ± 0.81 | 3.39–5.42 | 3.77 | 6.52 |
| La/Th | 6.01 ± 0.44 | 5.46–6.71 | 9.04 ± 0.84 | 7.12–10.9 | 5.85 | 6.48 |
| Zr/Hf | 39.1 ± 2.1 | 35.5–42.5 | 42.1 ± 4.4 | 36.5–50.8 | 39.6 | 50.3 |
| Hf/Ta | 10.54 ± 0.64 | 9.50–11.33 | 9.44 ± 1.46 | 7.22–11.94 | 9.94 | 10.3 |
| $La_N/Yb_N$ | 8.8 ± 0.8 | 7.7–10.4 | 14.2 ± 1.9 | 9.37–17.2 | 7.81 | 8.44 |
| Eu/Eu* | 1.02 ± 0.08 | 0.95–1.18 | 0.94 ± 0.07 | 0.82–1.1 | 1.01 | 0.92 |

Major element data in wt%; trace element data in ppm, except as noted. All Fe as $Fe_2O_3$. Blank space: no data available.

[a]From Koeberl et al. (1998).

[b]From Koeberl et al. (1997).

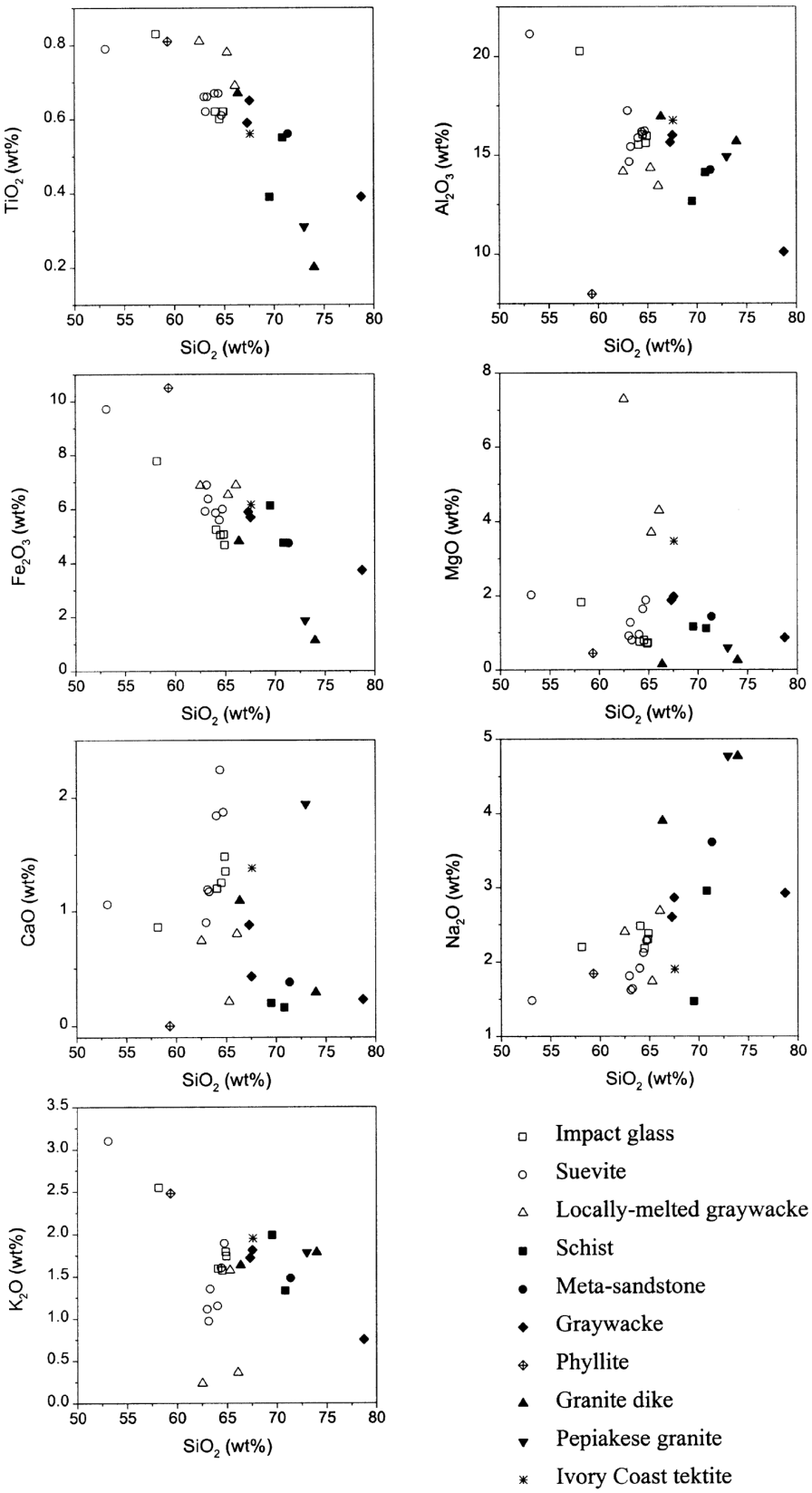


Fig. 2. A correlation of the contents of the major element oxides with silica abundances in Bosumtwi rocks (Table 2) compared to the average values for Ivory Coast tektites (after Koeberl et al. 1997).

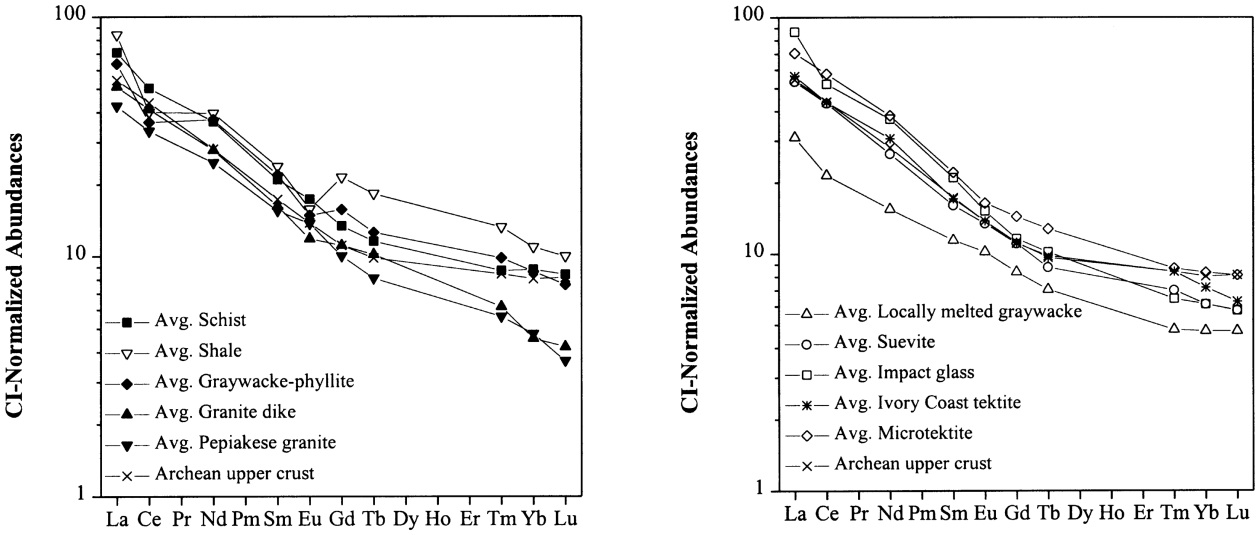


Fig. 3. A comparison of CI chondrite-normalized rare earth element distribution patterns for Bosumtwi rocks, Ivory Coast tektites and microtektites, and Archean upper crust. Averages of shale, graywacke-phyllite, granite dike, and Pepiakese granite from Koeberl et al. (1998); averages of Ivory Coast tektites and microtektites from Koeberl et al. (1997); Archean upper crustal values and normalization factors from Taylor and McLennan (1985).

indicative of either a chondritic or an iron meteoritic projectile (Koeberl 1998). If the meteoritic contribution is >0.1%, it is even possible to distinguish between chondritic and iron meteoritic contributions by evaluation of the Cr abundances and the Ni/Cr or Co/Cr ratios. This is possible because chondrites have high abundance of Cr, and low Ni/Cr or Co/Cr ratios, whereas iron meteorites have Cr abundances that are much more variable, but typically 100 times lower than those of chondrites (e.g., Palme et al. 1978; Evans et al. 1993; Koeberl 1998).

Based on high Ir and Os abundances in two Ivory Coast tektites analyzed by RNAA, Palme et al. (1978, 1981b) suspected that impact of an iron projectile might have generated the Bosumtwi crater. Koeberl and Shirey (1993) determined $^{187}Os/^{188}Os$ ratios of the Ivory Coast tektites, which are compatible with those in both carbonaceous chondrites and iron meteorites and also indicate that the terrestrial fraction does not exceed 10–20% of the total Os in the tektites. In contrast to the Bosumtwi target rocks, the Cr enrichment in the tektites seems to favor a chondritic projectile (see the Cr isotopic study of Koeberl et al. 2004). The high but variable Cr, Co, and Ni abundances in Bosumtwi target rocks that were determined in this study allow neither the unambiguous detection of a meteoritic component in Bosumtwi impactites nor the identification of the projectile type (chondrite or iron meteorite) (see Tables 2a, 2b, and 3). We emphasize that we do not conclude that Bosumtwi was formed by an iron projectile; rather that the present data do not allow to distinguish between chondritic and iron meteorite components because of the high and variable indigenous component.

The fact that the so-called "locally melted graywacke" samples yield near-chondritic Pd/Ru and Os-Ir ratios raises

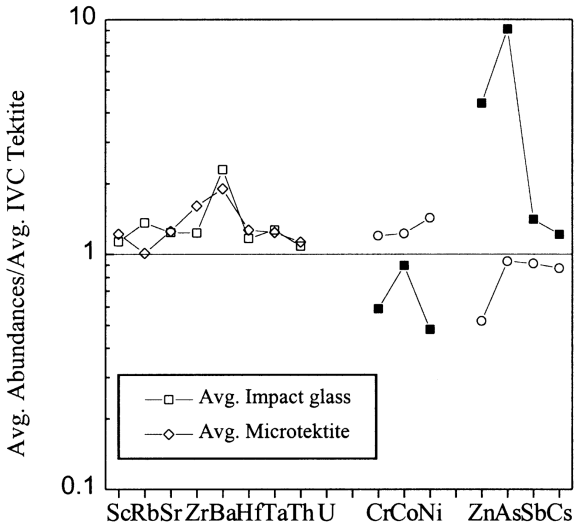


Fig. 4. A comparison of trace element abundances (in three groups: lithophile, siderophile, and volatile elements) of the averages for Ivory Coast tektites and microtektites (Koeberl et al. 1997) and Bosumtwi impact glasses.

the question about the nature and the origin of these materials. Texturally, these samples have been described variably as local granophyric granitoid melt rocks (Reimold et al. 1998) and as locally melted graywacke. No evidence of shock metamorphism has been observed in minerals of this material. It occurs in the form of decimeter to half-meter wide dikes cutting across various meta-sedimentary rock types in the crater rim. If it should be confirmed in the future that these dikes do indeed carry a meteoritic component, then their origin as impact breccia that was injected into the inner crater rim, which can not be excluded after these first

Table 4. Analytical data for PGEs, Au, Ag, and Re in Bosumtwi rocks determined by NAA and USN-ICP-MS after anion exchange preconcentration (ppb).

| Sample No. | Sample type | Ru | Pd | Ag | Re | Os | Ir | Pt | Au |
|---|---|---|---|---|---|---|---|---|---|
| LB-6 | Schist | 0.4 | 1.6 | 1.6 | 0.07 | 0.19 | 0.46 | 5.2 | 10.3 |
| LB-7 | Schist | 0.8 | 1.7 | 4.5 | 0.12 | 0.23 | 0.78 | 12 | 3.8 |
| LB-8 | Meta-sandstone | 0.4 | 1.4 | 4.4 | 0.07 | 0.33 | 0.53 | 12 | 7.8 |
| LB-12 | Graywacke | 0.3 | 1.5 | 3.7 | 0.10 | 0.35 | 0.63 | 5.2 | 2.6 |
| LB-17 | Graywacke | 0.4 | 1.1 | 5.4 | 0.18 | 0.19 | 0.49 | 57 | 9.4 |
| LB-19 | Locally melted graywacke | 1.0 | 1.5 | 6.0 | 0.061 | 0.54 | 0.50 | 3.5 | 4.1 |
| LB-21 | Locally melted graywacke | 0.7 | 0.6 | 13 | 0.045 | 0.38 | 0.42 | 14 | 8.2 |
| LB-25 | Locally melted graywacke | 1.9 | 0.9 | 15 | 0.08 | 0.34 | 0.35 | 4.4 | 3.2 |
| LB-27 | Quartzite | 1.3 | 3.2 | 5.1 | 0.22 | 0.22 | 0.29 | 1.5 | 0.63 |
| LB-28 | Granite dike | 3.0 | 2.0 | 10 | 0.079 | | 0.60 | 12 | 6.6 |
| LB-35 | Pepiakese granite | 1.3 | 0.8 | 8.4 | 0.045 | | 3.70 | 39 | 12.4 |
| LB-30 | Impact glass | 2.0 | 3.1 | 21 | 0.079 | 0.56 | 0.51 | 8.0 | 8.0 |
| LB-31A-E | Impact glass | 2.0 | 3.7 | 94 | 0.17 | 0.38 | 0.42 | 6.8 | 27.4 |
| LB-31A-F | Impact glass | 2.1 | 3.4 | 56 | 0.12 | 1.37 | 1.04 | 32 | 4.1 |
| LB-31A-G | Impact glass | 1.3 | 3.2 | 71 | 0.077 | 1.00 | 0.90 | 8.8 | 5.6 |
| LB-31A-H | Impact glass | 1.7 | 2.7 | 136 | 0.13 | 0.99 | 1.12 | 5.2 | 21.4 |
| WMG-1 | Reference material | 38.2 | 388 | 1800 | 2.6 | 11.8 | 48.4 | 673 | 120 |
| WMG-1 | Reference material | 30.2 | 346 | 1980 | 3.4 | 22.3 | 43.7 | 713 | 40 |
| | Literature values | 35 ± 5 | 382 ± 13 | | | 24 | 46 ± 4 | 731 ± 35 | 110 ± 11 |
| WITS-1 | Reference material | 4.9 | 6.5 | 6.66 | 0.13 | 0.69 | 1.44 | 11.1 | 15.8 |
| WITS-1 | Reference material | 4.7 | 7.2 | 7.02 | 0.058 | 0.99 | 1.98 | 9.9 | 6.2 |
| | Literature values | 5.1 ± 1.2 | 5.1 ± 1.2 | | 0.063[a] | 1 | 1.6 ± 0.2 | 11 ± 2.0 | 5.6 ± 1.8 |
| Blank | | 0.04 | 0.05 | 0.1 | 0.006 | 0.04 | 0.005 | 0.5 | 0.6 |

Ir, Au, Os, and Re measured by NAA; Ru, Pt, and Pd by USN-ICP-MS; Ag data are averages of NAA and USN-ICP-MS; blank spaces: no data available; reference values for standards WMG-1 from CANMET report CCRMP 94-1E and for WITS-1 from Tredoux and McDonald (1996).
[a]Information value from Pearson and Woodland (2000).

Table 5. Contents of Ru, Rh, Pd, Ir, Pt, and Au in other Bosumtwi rocks determined by ICP-MS after NiS fire assay preconcentration (ppb).

| Sample No. | Sample type | Ru | Rh | Pd | Ir | Pt | Au |
|---|---|---|---|---|---|---|---|
| LB-22 | Graywacke | 0.41 ± 0.10 | 0.23 ± 0.04 | 3.3 ± 0.4 | 0.25 ± 0.06 | 2.4 ± 1.0 | 1.0 ± 0.2 |
| LB-36 | Granite | 0.12 ± 0.03 | 0.08 ± 0.02 | 0.96 ± 0.30 | <0.03 | 0.72 ± 0.17 | 0.33 ± 0.07 |
| LB-37 | Phyllite | 0.24 ± 0.04 | 0.13 ± 0.02 | 1.2 ± 0.1 | 0.20 ± 0.02 | 1.7 ± 0.2 | 1.3 ± 0.1 |
| LB-30a | Suevite | 0.24 ± 0.05 | 0.13 ± 0.03 | 1.3 ± 0.1 | 0.25 ± 0.06 | 1.0 ± 0.2 | 3.0 ± 0.4 |
| LB-30b | Suevite | 0.34 ± 0.08 | 0.15 ± 0.04 | 1.6 ± 0.2 | 0.43 ± 0.05 | 1.6 ± 0.1 | 2.5 ± 0.1 |
| LB-41 | Suevite | 0.18 ± 0.06 | 0.12 ± 0.04 | 1.4 ± 0.2 | 0.19 ± 0.04 | 0.98 ± 0.10 | 5.7 ± 0.2 |

PGE analytical results presented here, would be confirmed. However, more geologic, petrographic, and geochemical data are needed to confirm this finding and to better constrain the still limited knowledge about the origin of these enigmatic materials.

**Mineralized Samples**

The mineralized samples are from the same stratigraphic interval that comprises the target rocks at the Bosumtwi crater. The town of Obuasi, where the Ashanti and the Tarkwa mines are located, is about 35 km from Bosumtwi. Detailed information on the mines and the mineralization is given by, e.g., Oberthür et al. (1994) and Osae et al. (1995). The compositions of the analyzed samples are given in Table 6. The major element compositions of the mineralized samples are more variable and, with the exception of the quartz-pebble conglomerate samples, they are Si-poor compared to the target rocks at Bosumtwi. Contents of Cr, Co, and Ni are within the same range as in the Bosumtwi target rocks. In terms of the PGE contents, however, there are some differences. Iridium contents are consistently low in all mineralized samples, ranging from 0.004 to 0.08 ppb—lower than the Ir contents of any of the analyzed rocks (target rocks and impactites) from Bosumtwi. The chondrite-normalized abundance patterns of the mineralized samples are shown in Fig. 8. It is immediately apparent that the patterns look different from those of the Bosumtwi rocks. The mineralized samples show positive Ru and Pt anomalies, possibly due to the presence of grains of laurite (RuS2) or Pt-Fe alloy in some samples, and of course most have much higher Au contents. We conclude that rocks similar to those from the Ashanti and Tarkwa mines were not sampled in the Bosumtwi area, possibly were not present, and apparently are not responsible for the high PGE contents of the Bosumtwi target rocks and impactites.

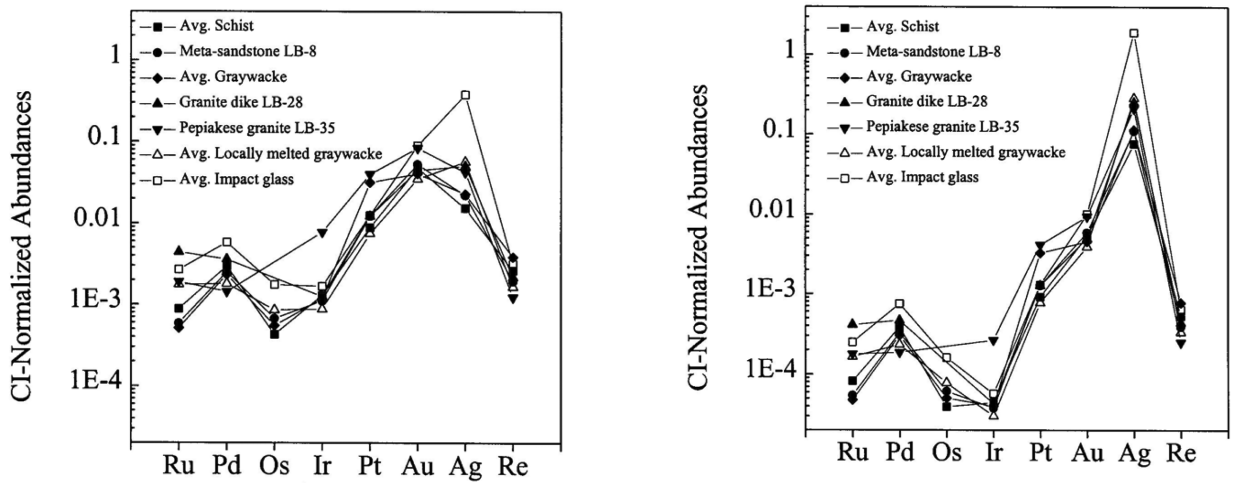


Fig. 5. a) CI chondrite and b) iron meteorite-normalized abundances of platinum group elements, Au, Ag, and Re in Bosumtwi crater rocks. Normalization factors for CI-chondritic values from Palme et al. (1981) and for IIIAB iron meteorite Cape York from Koeberl et al. (1986).

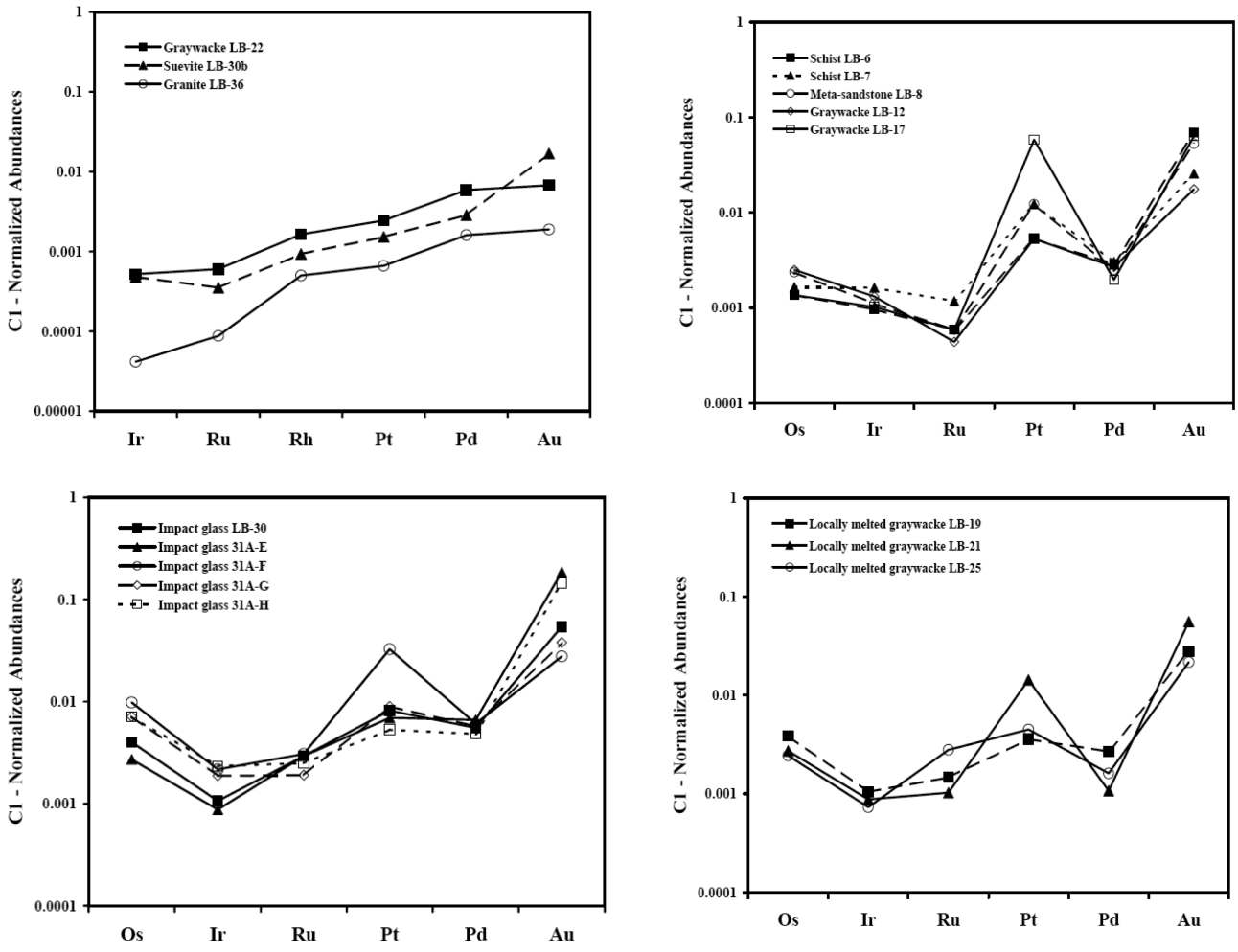


Fig. 6. Chondrite-normalized PGE abundance patterns for various Bosumtwi rocks. Normalization data from Jochum (1996), except for Pd, which is from Anders and Grevesse (1989). Data from Tables 4 and 5.

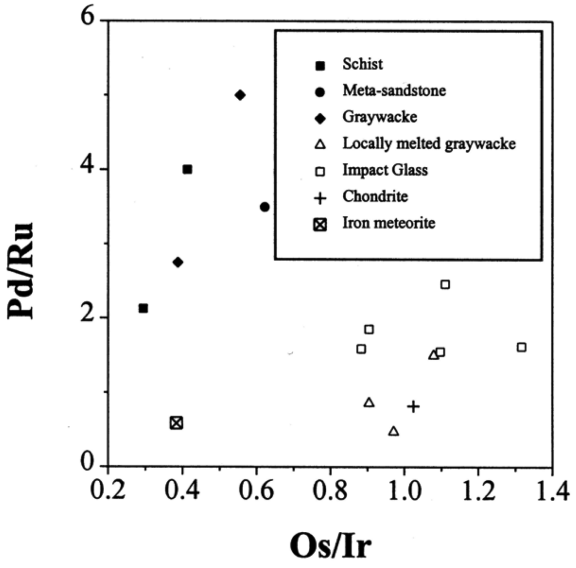


Fig. 7. Pd/Ru versus Os/Ir for Bosumtwi target rocks, impact glass, suevite, and "locally melted graywacke" compared to CI chondrite value (Palme et al. 1981).

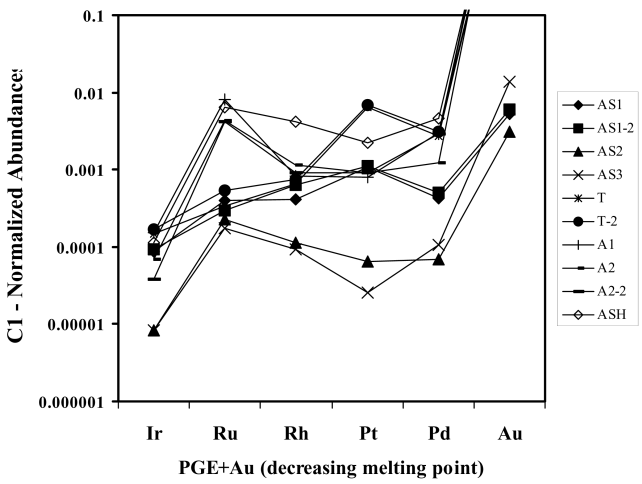


Fig. 8. Chondrite-normalized PGE abundance patterns for mineralized samples from the Ashanti and Tarkwa mines near Obuasi, Ghana. Normalization data from Jochum (1996), except for Pd, which is from Anders and Grevesse (1989).

## CONCLUSIONS

A set of target rocks and impactites from the Bosumtwi crater (Ghana), as well as some mineralized samples from further away from the crater but involving the same stratigraphic section of the Tarkwaian Supergroup that could have been part of the target geology at Bosumtwi, were analyzed for their major and trace element composition, especially platinum group element abundances, as well as their petrographic characteristics. Very similar CI chondrite-normalized REE abundance patterns, which are characterized by the lack of an appreciable Eu anomaly and total REE concentrations similar to Archean upper crust, were observed for Bosumtwi target rocks as well as impactites, and for Ivory Coast tektites and microtektites. With regard to lithophile element abundances, Bosumtwi impact glass and Ivory Coast tektites are very similar. In contrast, the abundances of siderophile elements are lower in Bosumtwi impact glass than in the tektites, and a number of volatile elements are comparatively enriched in the impact glass. The overall comparison of geochemical characteristics of Bosumtwi target rocks, impact glass, and suevite, as well as Ivory Coast tektites, supports previous results that the Bosumtwi impact structure represents the origin of the Ivory Coast tektites and microtektites.

However, some distinct differences between chemical compositions of Bosumtwi impact glass and Ivory Coast tektites exist (e.g., higher MgO, Zn, and As, and lower Cr, Co, Ni, and Au contents in the impact glasses), similar to chemical differences between moldavites and impact glasses at the Ries impact structure, Germany (see Koeberl 1994 for a review).

Platinum group element analysis was applied in an attempt to identify a possible extraterrestrial component in impactites from Bosumtwi crater. In agreement with previous studies (e.g., Koeberl and Shirey 1993), the abundances of the PGEs and other siderophile elements in the target rocks were found to be elevated compared to average upper crustal abundances. Despite some high values for Ir and other PGEs in a few of the suevite samples, the presence of a meteoritic component in Bosumtwi impactites could not be distinguished on the basis of siderophile element analysis due to the overlap of the target rocks and impactite PGE abundances. There is only a hint for the presence of a meteoritic contribution in Bosumtwi impactites in the Pd/Ru and Os/Ir interelement ratios, which are, in part, close to chondritic values. A similar signature determined for the enigmatic dike samples ("locally melted graywacke") is puzzling and demands further dedicated study of these dike materials. In agreement with Jones (1985), Koeberl and Shirey (1993), and Koeberl et al. (1998), we assume that the relatively high siderophile element abundances in the target lithologies are related to the gold mineralization present in this region of the Ashanti Province. However, the PGE abundance patterns in the ore mineralized samples from the Ashanti and Tarkwa mines, about 35 and 50 km from Bosumtwi in the same type host rocks as at Bosumtwi, are quite different from those of the Bosumtwi rocks. Abundances of Ir in the ore mineralized samples are significantly lower, and those of Rh and Au significantly higher, than in the Bosumtwi rocks. Thus, we conclude that some other local indigenous mineralization at or near Bosumtwi may have been responsible for the high PGE contents in the Bosumtwi rocks, and the PGE abundances and patterns do not provide an unambiguous answer regarding the presence and identity of a meteoritic

Table 6. Chemical compositions of mineralized samples from the Ashanti and Tarkwa mines (Obuasi, Ghana).

| | Quartz mica schist | | Amphibolites | | | | | | Quartz-pebble conglomerates | |
|---|---|---|---|---|---|---|---|---|---|---|
| | A1 | A2 | A2-2 | ASH | AS1 | AS1-2 | AS2 | AS3 | T | T-2 |
| (wt%) | | | | | | | | | | |
| $SiO_2$ | 42.94 | 64.77 | 62.12 | 46.28 | 47.18 | 48.12 | 45.56 | 51.13 | 86.40 | 85.43 |
| $TiO_2$ | 0.99 | 0.56 | 0.62 | 0.81 | 0.81 | 0.87 | 0.80 | 1.10 | 0.30 | 0.34 |
| $Al_2O_3$ | 28.09 | 12.76 | 14.11 | 21.35 | 14.10 | 15.11 | 16.26 | 16.05 | 2.98 | 2.76 |
| $Fe_2O_3$ | 0.94 | 5.28 | 5.82 | 7.89 | 14.08 | 13.67 | 11.55 | 12.25 | 7.82 | 7.96 |
| MnO | 0.01 | 0.10 | 0.08 | 0.07 | 0.20 | 0.19 | 0.17 | 0.19 | 0.16 | 0.15 |
| MgO | 0.27 | 1.80 | 1.95 | 2.14 | 6.93 | 6.84 | 6.89 | 5.35 | 0.06 | 0.08 |
| CaO | 13.43 | 2.36 | 2.45 | 2.77 | 11.67 | 10.32 | 7.85 | 9.94 | 1.06 | 1.11 |
| $Na_2O$ | 2.04 | 0.97 | 1.06 | 1.63 | 1.69 | 1.76 | 1.80 | 1.96 | 0.26 | 0.24 |
| $K_2O$ | 0.25 | 2.82 | 2.97 | 4.54 | 0.02 | 0.12 | 0.08 | 0.32 | 0.30 | 0.32 |
| $P_2O_5$ | 0.01 | 0.06 | 0.05 | 0.05 | 0.05 | 0.09 | 0.10 | 0.12 | 0.07 | 0.06 |
| L.O.I | 11.05 | 7.60 | 7.89 | 11.62 | 2.24 | 2.87 | 8.04 | 0.79 | 0.62 | 0.75 |
| Total | 100.02 | 99.08 | 99.12 | 99.15 | 98.97 | 99.96 | 99.10 | 99.20 | 100.03 | 99.20 |
| (ppm) | | | | | | | | | | |
| V | 183 | 86 | 98 | 147 | 271 | 243 | 146 | 205 | 161 | 151 |
| Cr | 68 | 49 | 43 | 26 | 382 | 256 | 84 | 103 | 98 | 91 |
| Co | 11 | 12 | 16 | 37 | 49 | 46 | 56 | 42 | 16 | 12 |
| Ni | 37 | 22 | 28 | 65 | 162 | 111 | 57 | 19 | 11 | 12 |
| Cu | 51 | 69 | 62 | 43 | 115 | 87 | 39 | 44 | 14 | 10 |
| Zn | 118 | 82 | 78 | 67 | 85 | 85 | 83 | 87 | 17 | 18 |
| Rb | 169 | 124 | 134 | 163 | 10 | 8 | 6 | 16 | 9 | 8 |
| Sr | 424 | 233 | 289 | 496 | 223 | 289 | 457 | 256 | 71 | 65 |
| Y | 33 | 18 | 18 | 20 | 20 | 23 | 25 | 30 | 12 | 14 |
| Zr | 189 | 130 | 150 | 170 | 50 | 71 | 66 | 88 | 183 | 198 |
| Nb | 12 | 9 | 10 | 10 | 6 | 6 | 5 | 6 | 6 | 5 |
| Ba | 938 | 509 | 587 | 752 | 47 | 87 | 49 | 356 | 817 | 756 |
| (ppb) | | | | | | | | | | |
| Ir | 0.074 | 0.033 | 0.018 | 0.054 | 0.042 | 0.044 | 0.004 | 0.004 | 0.072 | 0.080 |
| Ru | 5.480 | 2.960 | 2.845 | 4.435 | 0.271 | 0.205 | 0.154 | 0.119 | 0.233 | 0.365 |
| Rh | 0.115 | 0.161 | 0.126 | 0.588 | 0.058 | 0.090 | 0.016 | 0.013 | 0.092 | 0.105 |
| Pt | 0.785 | 0.906 | 0.895 | 2.210 | 1.068 | 1.103 | 0.063 | 0.025 | 6.431 | 6.755 |
| Pd | 1.659 | 0.690 | 1.640 | 2.540 | 0.238 | 0.285 | 0.038 | 0.060 | 1.533 | 1.712 |
| Au | 5521 | 7136 | 7350 | 4863 | 0.781 | 0.883 | 0.456 | 2.058 | 2737 | 2560 |

Note: All Fe as $Fe_2O_3$.

component. In addition, differences between some of the results obtained by different analytical procedures complicate the interpretation of the results even further. More detailed isotopic studies (Cr and Os isotopes) of the various rocks at Bosumtwi (impact breccias as well as target rocks) will be necessary to resolve this issue, and to compare with the positive Os and Cr isotopic results obtained for Ivory Coast tektites (Koeberl and Shirey 1993; Koeberl et al. 2004).

The problems encountered in the present study may serve as a warning for similar attempts to investigate possible meteoritic projectile traces at other impact structures where the siderophile element contribution from the target rocks is not fully understood.

*Acknowledgments*–We are grateful to the Geological Survey of Ghana for logistical support. This research was supported by the Austrian FWF, project 17194-N10 (to C. Koeberl). The support of the Austrian Academic Exchange Service (to X. Dai and D. Boamah) is also appreciated. W. U. Reimold's research is supported by the South African National Research Foundation and the Research Council of the University of the Witwatersrand. We greatly appreciate R. Klemd (University of Würzburg, Germany) for supplying the ore mineralized samples from the Ashanti and Tarkwa mines and corresponding mineralogical descriptions. We are also grateful to Heinz Huber (then at the University of Vienna), Heinz Fröschl (Arsenal Research, Vienna), and Max Bichler (Atominstitut, Vienna) for technical assistance, and to Ross Taylor (The Australian National University) for valuable discussions. We appreciate helpful and critical reviews by P. Claeys and R. Tagle, and editorial comments by U. Riller. This is University of the Witwatersrand Impact Cratering Research Group Contribution No. 89.

*Editorial Handling*—Dr. Ulrich Riller

## REFERENCES


Anders E. and Grevesse N. 1989. Abundances of the elements: Meteoritic and solar. *Geochimica et Cosmochimica Acta* 53:197–214.

Boamah D. and Koeberl C. 2002. Geochemistry of soils from the Bosumtwi impact structure, Ghana, and relationship to radiometric airborne geophysical data. In *Meteorite impacts in Precambrian shields,* edited by Plado J. and Pesonen L. Impact Studies, vol. 2. Heidelberg-Berlin: Springer. pp. 211–255.

Boamah D. and Koeberl C. 2003. Geology and geochemistry of shallow drill cores from the Bosumtwi impact structure, Ghana. *Meteoritics & Planetary Science* 38:1137–1159.

CANMET (Energy, Mines and Resources Canada) report CCRMP (Canadian Certified Reference Materials Project) 94-1E. 68 p.

Colodner D. C., Boyle E. A., and Edmond J. M. 1993. Determination of rhenium and platinum in natural waters and sediments and iridium in sediments by flow injection isotope dilution inductive coupled plasma mass spectrometry. *Analytical Chemistry* 65: 1419–1425.

Crocket J. H., Keays R. R., and Hsieh S. 1968. Determination of some precious metals by neutron activation analysis. *Journal of Radioanalytical Chemistry* 1:487–507.

Dai X., Chai Z., Mao X., Wang J., Dong S., and Li K. 2000. An α-amino pyridine resin preconcentration method for iridium in environmental and geological samples. *Analytica Chimica Acta* 403:243–247.

Dai X., Koeberl C., and Fröschl H. 2001. Determination of platinum group elements in impact breccias using neutron activation analysis and ultrasonic nebulization inductively coupled plasma mass spectrometry after anion exchange preconcentration. *Analytica Chimica Acta* 436:79–85.

El Goresy A. 1966. Metallic spherules in Bosumtwi crater glasses. *Earth and Planetary Science Letters* 1:23–24.

Evans N. J., Gregoire D. C., Grieve R. A. F., Goodfellow W. D., and Veizer J. 1993. Use of platinum-group elements for impactor identification: Terrestrial impact craters and Cretaceous-Tertiary boundary. *Geochimica et Cosmochimica Acta* 57:3737–3748.

Hirdes W. and Nunoo B. 1994. The Proterozoic palaeoplacers at Tarkwa gold mine/SW Ghana—Sedimentology, mineralogy, and precise age dating of the Main Reef and West Reef, and bearing of the investigations on source area aspects. *Geologisches Jahrbuch D* 100:247–311.

Huber H., Koeberl C., McDonald I., and Reimold W. U. 2001. Geochemistry and petrology of Witwatersrand and Dwyka diamictites from South Africa: Search for an extraterrestrial component. *Geochimica et Cosmochimica Acta* 65:2007–2016.

Jarvis I., Totland M. M., and Jarvis K. E. 1997. Assessment of Dowex 1-X8-based anion-exchange procedures for the separation and determination of ruthenium, rhodium, palladium, iridium, platinum, and gold in geological samples by inductively coupled plasma mass spectrometry. *Analyst* 122:19–26.

Jochum K. 1996. Rhodium and other platinum-group elements in carbonaceous chondrites. *Geochimica et Cosmochimica Acta* 60: 3353–3357.

Jones W. B. 1985. Chemical analyses of Bosumtwi crater target rocks compared with the Ivory Coast tektites. *Geochimica et Cosmochimica Acta* 48:2569–2576.

Jones W. B., Bacon M., and Hastings D. A. 1981. The Lake Bosumtwi impact crater, Ghana. *Geological Society of America Bulletin* 92:342–349.

Junner N. R. 1937. The geology of the Bosumtwi caldera and surrounding country. *Gold Coast Geological Survey Bulletin* 8: 1–38.

Karp T., Milkereit B., Janle J., Danuor S. K., Pohl J., Berckhemer H., and Scholz C. A. 2002. Seismic investigation of the Lake Bosumtwi impact crater: Preliminary results. *Planetary and Space Science* 50:735–743.

Koeberl C. 1993. Instrumental neutron activation analysis of geochemical and cosmochemical samples: A fast and proven method for small sample analysis. *Journal of Radioanalytical and Nuclear Chemistry* 168:47–60.

Koeberl C. 1994. Tektite origin by hypervelocity asteroidal or cometary impact: Target rocks, source craters, and mechanisms. In *Large meteorite impacts and planetary evolution,* edited by Dressler B. O., Grieve R. A. F., and Sharpton V. L. GSA Special Paper #293. Boulder, Colorado: Geological Society of America. pp. 133–152.

Koeberl C. 1998. Identification of meteoritic components in impactites. In *Meteorites: Flux with time and impact effects,* edited by Grady M. M., Hutchison R., McCall G. J. H., and Rothery D. A. London: The Geological Society. pp. 133–153.

Koeberl C. and Reimold W. U. 2005. Bosumtwi impact crater, Ghana (West Africa): An updated and revised geological map, with explanations. *Jahrbuch der Geologischen Bundesanstalt* (Vienna, Austria) (Yearbook of the Geological Survey of Austria) 145:31–70 (with one map).

Koeberl C. and Shirey S. B. 1993. Detection of a meteoritic component in Ivory Coast tektites with rhenium-osmium isotopes. *Science* 261:595–598.

Koeberl C. and Shirey S. B. 1997. Re-Os isotope systematics as a diagnostic tool for the study of impact craters and distal ejecta. *Palaeogeography, Palaeoclimatology, Palaeoecology* 132:25–46.

Koeberl C., Weinke H. H., Kluger F., and Kiesl W. 1986. Cape York IIIAB iron meteorite: Trace element distribution in mineral and metallic phases. *Proceedings of the Tenth Symposium on Antarctic Meteorites*. pp. 297–313.

Koeberl C., Bottomley R. J., Glass B. P., and Storzer D. 1997. Geochemistry and age of Ivory Coast tektites and microtektites. *Geochimica et Cosmochimica Acta* 61:1745–1772.

Koeberl C., Reimold W. U., Blum J. D., and Chamberlain C. P. 1998. Petrology and geochemistry of target rocks from the Bosumtwi impact structure, Ghana, and comparison with Ivory Coast tektites. *Geochimica et Cosmochimica Acta* 62:2179–2196.

Koeberl C., Reimold W. U., McDonald I., and Rosing M. 2000. Search for petrographic and geochemical evidence for the late heavy bombardment on Earth in early Archean rocks from Isua, Greenland. In *Impacts and the early Earth,* edited by Gilmour I. and Koeberl C. Heidelberg-Berlin: Springer. pp. 73–97.

Koeberl C., Shukolyukov A., and Lugmair G. 2004. An ordinary chondrite impactor composition for the Bosumtwi impact structure, Ghana, West Africa: Discussion of siderophile element contents and Os and Cr isotope data (abstract #1256). 35th Lunar and Planetary Science Conference. CD-ROM.

Koeberl C., Milkereit B., Overpeck J. T., Scholz C. A., Peck J., and King J. 2005. The 2004 ICDP Bosumtwi impact crater, Ghana, West Africa, drilling project: A first report (abstract #1830). 36th Lunar and Planetary Science Conference. CD-ROM.

Kolbe P., Pinson W. H., Saul J. M., and Miller E. W. 1967. Rb-Sr study on country rocks of the Bosumtwi crater, Ghana. *Geochimica et Cosmochimica Acta* 31:869–875.

Leube A., Hirdes W., Mauer R., and Kesse G. O. 1990. The Early Proterozoic Birimian Supergroup of Ghana and some aspects of its associated gold mineralization. *Precambrian Research* 46: 139–165.

Moon P. A. and Mason D. 1967. The geology of 1/4° field sheets 129 and 131, Bompata SW and NW. *Ghana Geological Survey Bulletin* 31:1–51.

Oberthür T., Vetter U., Schmidt-Mumm A., Weiser T., Amanor J. A., Gyapong W. A., Kumi R., and Blenkinsop T. G. 1994. The Ashanti gold mine at Obuasi, Ghana: Mineralogical,

geochemical, stable isotope, and fluid inclusion studies on the metallogenesis of the deposit. *Geologisches Jahrbuch D* 100:31–129.

Osae S., Kase K., and Yamamoto M. 1995. A geochemical study of the Ashanti gold deposit at Obuasi, Ghana. *Okayama University Earth Science Reports* 2:81–90.

Palme H., Janssens M. J., Takahasi H., Anders E., and Hertogen J. 1978. Meteorite material at five large impact craters. *Geochimica et Cosmochimica Acta* 42:313–323.

Palme H., Grieve R. A. F., and Wolf. R. 1981. Identification of the projectile at the Brent crater, and further considerations of projectile types at terrestrial craters. *Geochimica et Cosmochimica Acta* 45:2417–2424.

Palme H., Suess H. E., and Zeh H. D. 1981. Abundances of the elements in the solar system. In *Landolt-Boernstein,* vol. 2, subvol. A (Methods, Constants, Solar System), edited by Schaifers K. and Voigt H. H. Heidelberg: Springer pp. 257–273.

Pearson D. G. and Woodland S. J. 2000. Solvent extraction/anion exchange separation and determination of PGEs (Os, Ir, Pt, Pd, Ru) and Re-Os isotopes in geological samples by isotope dilution ICP-MS. *Chemical Geology* 165:87–107.

Peck J. A., Green R. R., Shanahan T., King J. W., Overpeck J. T., and Scholz C. A. 2004. A magnetic mineral record of Late Quaternary tropical climate variability from Lake Bosumtwi, Ghana. *Palaeogeography, Palaeoclimatology, Palaeoecology* 215:37–57.

Pernicka E., Kaether D., and Koeberl C. 1996. Siderophile element concentrations in drill core samples from the Manson crater. In *The Manson impact structure, Iowa: Anatomy of an impact crater,* edited by Koeberl C. and Anderson R. R. GSA Special Paper #302. Boulder, Colorado: Geological Society of America. pp. 325–330.

Pesonen L. J., Koeberl C., and Hautaniemi H. 2003. Airborne geophysical survey of the Lake Bosumtwi meteorite impact structure (southern Ghana)—Geophysical maps with descriptions. *Jahrbuch der Geologischen Bundesanstalt* (Vienna, Austria) (Yearbook of the Geological Survey of Austria) 143: 581–604.

Plado J., Pesonen L. J., Koeberl C., and Elo S. 2000. The Bosumtwi meteorite impact structure, Ghana: A magnetic model. *Meteoritics & Planetary Science* 35:723–732.

Reimold W. U., Koeberl C., and Bishop J. 1994. Roter Kamm impact crater, Namibia: Geochemistry of basement rocks and breccias. *Geochimica et Cosmochimica Acta* 58:2689–2710.

Reimold W. U., Brandt D., and Koeberl C. 1998. Detailed structural analysis of the rim of a large, complex impact crater: Bosumtwi crater, Ghana. *Geology* 26:543–546.

Scholz C. A, Karp T., Brooks K. M., Milkereit B., Amoako P. Y. A., and Arko J. A. 2002. Pronounced central uplift identified in the Lake Bosumtwi impact structure, Ghana, using multichannel seismic reflection data. *Geology* 30:939–942.

Taylor S. R. and McLennan S. M. 1985. *The continental crust: Its composition and evolution.* Oxford: Blackwell Science Publishers. 312 p.

Tredoux M. and McDonald I. 1996. Komatiite Wits-1, low concentration noble metal standard for the analysis of non-mineralized samples. *Geostandards Newsletter* 20:267–276.

Wagner R., Reimold W. U., and Brandt D. 2002. Bosumtwi impact crater, Ghana: A remote sensing investigation. In *Meteorite impacts in Precambrian shields,* edited by Plado J. and Pesonen L. J. Impact Studies, vol. 2. Heidelberg: Springer. pp. 189–210.

Woodfield P. D. 1966. The geology of the 1/4° field sheet 91, Fumso NW. *Ghana Geological Survey Bulletin* 30:1–66.

Wright J. B., Hastings D. A., Jones W. B., and Williams H. R. 1985. *Geology and mineral resources of West Africa.* Boston: Allen and Unwin. 187 p.

Yao Y. and Robb L. J. 1998. The Birimian granitoids of Ghana: A review. Economic Geology Research Unit Information Circular #322. University of the Witwatersrand, Johannesburg, South Africa. pp. 1–46.

Yi Y. V. and Masuda A. 1996. Simultaneous determination of ruthenium, palladium, iridium and platinum at ultratrace levels by isotope dilution inductively coupled plasma mass spectrometry in geological samples. *Analytical Chemistry* 68: 1444–1450.